
This is the **accepted version** of the journal article:

Piñero, Pedro; López García, Juan Manuel; Blain, Hugues-Alexandre; [et al.].
«Multiproxy approach to reconstruct the climate and environment of a new
late Middle Pleistocene vertebrate site in northwestern Italy». *Palaeogeography,
Palaeoclimatology, Palaeoecology*, Vol. 634 (January 2024), art. 111935. DOI
10.1016/j.palaeo.2023.111935

This version is available at <https://ddd.uab.cat/record/301273>

under the terms of the  license

1 **Multiproxy approach to reconstruct the climate and environment of a**
2 **new late Middle Pleistocene vertebrate site in northwestern Italy**

3 Pedro Piñero^{a,b,*}, Juan Manuel López-García^{a,b}, Hugues-Alexandre Blain^{a,b}, Giorgio
4 Carnevale^c, Marc Furió^{d,e}, Piero Giuntelli^c, Elisa Luzi^f, Loredana Macaluso^c, Giuseppe
5 Marramà^c, Shubham Pal^{d,e}, Giulio Pavia^c, Marco Pavia^c, Claudia Pezzetti^c, Massimo
6 Rocca^c, Christian Sánchez-Bandera^{a,b}, Andrea Villa^e, Massimo Delfino^{c,e}

7 ^aInstitut Català de Paleoecologia Humana i Evolució Social (IPHES-CERCA), Zona
8 Educacional 4, Campus Sescelades URV (Edifici W3), 43007, Tarragona, Spain.

9 ^bÀrea de Prehistòria, Universitat Rovira i Virgili (URV), Avinguda de Catalunya 35,
10 43002, Tarragona, Spain.

11 ^cDipartimento di Scienze della Terra, Università degli Studi di Torino, via Valperga
12 Caluso 35, 10125 Turin, Italy.

13 ^dDepartament de Geologia, Universitat Autònoma de Barcelona, Cerdanyola del Vallès,
14 08193, Barcelona, Spain.

15 ^eInstitut Català de Paleontologia Miquel Crusafont (ICP-CERCA), Edifici ICTA-ICP, c/
16 Columnes s/n, Campus de la UAB, 08193 Cerdanyola del Vallès, Barcelona, Spain.

17 ^fInstitute for Archaeological Sciences (INA), University of Tübingen. Hölderlinstrasse
18 12, 72074 Tübingen (Germany).

19 * Corresponding author: ppinero@iphes.cat

20

21

22

23 ABSTRACT

24 The Moletto site (Ottiglio, AL, Piemonte, Italy) was discovered in the 1990s in an
25 abandoned quarry carved into a Burdigalian–Langhian carbonate succession called Pietra
26 da Cantoni. Sediment collection in three closely spaced fissures provided a rich vertebrate
27 association whose age can be constrained to the late Middle Pleistocene on the basis of
28 the presence of the extinct water vole *Arvicola mosbachensis* and its enamel
29 characteristics (SDQ values ranging from 100 to 130). The very similar faunal content,
30 evidenced by the common presence of *Arvicola mosbachensis* and its similar SDQ values,
31 is indicative of a coeval deposition of the fillings of the three fissures. The vertebrate
32 assemblage is represented by 30 taxa, including amphibians, squamate reptiles, birds, and
33 mammals. Interestingly, a diverse fish assemblage from the embedded sediments of the
34 Miocene Pietra da Cantoni has been found in the fissure fillings. We present here a multi-
35 method approach using the small vertebrate assemblages (rodents, insectivores,
36 amphibians, and squamate reptiles) from Moletto to characterise the environment and
37 climate of the site. In order to reconstruct the palaeoenvironmental and palaeoclimatic
38 conditions, we applied the Mutual Ecogeographic Range using UDA-ODA technique, the
39 Bioclimatic Model, the Habitat Weightings, and the Quantified Ecology methods. The
40 results revealed a landscape dominated by woodland habitats with presence of open
41 humid meadows, under temperate and moist climatic conditions, although somewhat
42 colder and drier than today. According to all evidence, the associations from Moletto
43 would correspond to the interglacial MIS 7.

44 **Keywords:** vertebrate assemblage; Mutual Ecogeographic Range; Bioclimatic Model;
45 Quantified Ecology; Habitat Weightings; Marine Isotope Stage 7.

46

47 **1. Introduction**

48 The late Middle Pleistocene and the early Late Pleistocene represent periods of
49 significant climatic variability. They could be included into the Marine Isotope Stages
50 (MIS) 7 to 5, culturally characterised by the Mousterian which is a Middle Palaeolithic
51 ensemble of Neanderthal-related techno-complexes in Europe. Climatic oscillations
52 affected small mammal faunas, as well as hominid groups, mainly through availability of
53 resources (Dennell et al., 2011). Studies on the Middle/Late Pleistocene fauna are
54 essential to provide a sound biochronology and to reconstruct palaeoenvironmental shifts
55 involving hominid migrations, population size changes and species turnover (Berto et al.,
56 2021).

57 Small vertebrates are particularly suited for biochronology and
58 palaeoenvironmental reconstructions. In the late Middle Pleistocene, at the boundary
59 between the early and late Toringian, a critical transition in the rodent fauna took place,
60 when *Arvicola mosbachensis* was replaced by *Arvicola amphibius* (Fejfar and Heinrich,
61 1988; Maul et al., 2000; Kalthoff et al., 2007; Berto et al., 2021).

62 The MIS 7 corresponds to the late Middle Pleistocene, being dated to ca. 246–186
63 ka. It is characterised by a marked alternation of three warm (MIS 7e, MIS 7c, and MIS
64 7a) and two cold episodes (MIS 7d and MIS 7b) (Desprat et al., 2006; Roucoux et al.,
65 2006, 2008; Railsback et al., 2015). It seems that during MIS 7, the Middle Palaeolithic
66 culture was established in Italy (Torre in Pietra site; Villa et al., 2016). In the Italian
67 Peninsula, terrestrial records based on small vertebrate studies from the late Middle
68 Pleistocene are limited to Torre in Pietra 2 in Latium (Caloi and Palombo, 1978), and
69 three localities in Berici Hills (Vicenza): the lower layers of Grotta del Broion (Sala,
70 1980; Colamussi, 2002), the lower units (Units VIII-VII) of Grotta Maggiore di San

71 Bernardino (López-García et al., 2017) and probably Sossano 2 (Bartolomei, 1980; Bon
72 et al., 1991).

73 The MIS 6 (ca. 185–135 ka) corresponds to the penultimate glacial period and to
74 the late Saalian glaciation in Europe (Ehlers et al., 2011). According to pollen data, the
75 early part of MIS 6 in Europe was marked by a moderately severe climate with fluctuating
76 tree abundances. This phase was followed by more extreme conditions characterised by
77 a mainly treeless environment at the end of the penultimate glacial (Roucoux et al., 2011).
78 However, there are very few palaeontological sites in southern Mediterranean Europe
79 documenting terrestrial faunas of the MIS 6 (Blain et al., 2017; López-García et al., 2021),
80 with one of them, Poggetti Vecchi (Benvenuti et al., 2017), located in Italy.

81 The MIS 5, dated to ca. 130 to 75 ka (early Late Pleistocene), represents a stage of
82 minimum ice volume. It includes three warm phases (MIS 5e, MIS 5c, and MIS 5a)
83 alternating with two cold phases (MIS 5d and MIS 5b) (Kukla et al., 2002; Sánchez-Goñi
84 et al., 2012; among others). Again, the continental record with small vertebrate surveys
85 for MIS 5 in Italy is scarce, being limited to Ciota Ciara cave in Borgosesia (Berto et al.,
86 2016), upper layers of Caverna degli Orsi in Trieste (Berto and Rubinato, 2013), and Unit
87 V of Grotta Maggiore di San Bernardino (López-García et al., 2017).

88 Here, the vertebrate assemblage from the site of Moleto (northwestern Italy) is
89 presented in order to help to expand our knowledge on the faunistic context of the late
90 Middle to early Late Pleistocene in northern Italy. Considering the small mammal
91 assemblage, a chronological approach of the sites has been performed, putting it in
92 relation to a broad context. In addition, an environmental and climatic reconstruction of
93 Moleto has been carried out using a set of methods applied to small mammals and
94 herpetofauna to shed light on the landscape and climate prevailing in the studied region
95 at the end of the Middle Pleistocene.

96 2. Site

97 The Moleto site is formed by a set of fissures filled by sediments of Middle/Late
98 Pleistocene age. It is located near the small town of Moleto (Ottiglio Monferrato,
99 Piedmont region, Northwest Italy; Fig. 1A), at an altitude between 187 and 207 m.a.s.l.
100 The location coordinates are 45° 1' 42" N, 8° 13' 12" E. The Monferrato area (southeastern
101 Piedmont) is part of the Tertiary Piedmont Basin, a marine sedimentary basin formed
102 during the Cenozoic (late Eocene–Late Miocene), and is characterised by two separate
103 stratigraphic successions cropping out in western and eastern sections, respectively. The
104 eastern Monferrato sequence (Oligocene–Late Miocene) is made up of terrigenous
105 deposits of variable thickness, overlain by shallow-water shelf carbonates (Mancin et al.,
106 2003). These include different units, among which the Pietra da Cantoni Formation
107 occupies the uppermost portion (Tosetto et al., 2023). The Moleto site was discovered in
108 the 1990s in an abandoned quarry carved into a Burdigalian–Langhian carbonate
109 succession of the Pietra da Cantoni Formation (Bonsignore et al., 1969; Clari et al., 1994;
110 Roggero, 2003).

111 Remarkably, a diverse fish assemblage including squalomorph and galeomorph
112 sharks, batoids, and percomorph bony fishes reworked from the embedded sediments of
113 the Miocene Pietra da Cantoni, and indicative of shallow to deep shelf marine biotopes,
114 has been found in the fissure fillings (see supplementary material 1).

115 The Moleto site hosts three closely spaced fissures with palaeontological content:
116 Moleto 0, Moleto 1, and Moleto 2. All the deposits filling the three fissures have the same
117 sedimentary source. In addition, their very similar faunal content, evidenced by the
118 common presence of *Arvicola mosbachensis* and its similar SDQ values (as discussed
119 below), is indicative of a coeval sediment deposition of the three localities, which are
120 considered as a single assemblage in the following analyses.

121 Moleto 0 is 1.5 m wide and 0.2 to 0.4 m thick (Fig. 1C) and consists of a
122 conglomerate with centimetric to pluricentimetric pebbles of Pietra da Cantoni carbonates
123 in a reddish-brown sandy clay matrix with well-thickened Mn and Fe oxides. Small
124 vertebrate remains are relatively abundant. This fissure has also yielded some large
125 mammal remains.

126 Moleto 1 is 1.3 m thick and up to 0.85 m wide (Fig. 1B). The fissure is rich in small
127 vertebrates, but limited in large mammals. It can be subdivided from the base to the top
128 into six levels of variable thickness: Level 6 (10–15 cm), Level 5 (15–20 cm), Level 4
129 (10–15 cm), Level 3 (20–25 cm), Level 2 (~30 cm), and Level 1 (30–35 cm). Level 6
130 consists of reddish silty sands, with some pebbles and abundant carbonaceous residues
131 and oxides of Mn and Fe, with the base more conglomeratic, including centimetric,
132 moderately rounded pebbles of Pietra da Cantoni carbonates. Microvertebrates are
133 abundant. Level 5 is formed by slightly pebbly silty sands, with dark green clays and
134 oxides of Mn and Fe. It has yielded microvertebrates remains. Level 4 consists of silt with
135 red-brown sands, lacking lamination. Fossils are absent. Level 3 is composed of yellow
136 ochraceous silts, slightly sandy and densely laminated. There are pockets of sandy,
137 reddish-brown sediment with microvertebrates. Level 2 consists of reddish-brown sandy
138 silts, with pockets of dark brown sandy sediment. Fossils are present. The non-
139 fossiliferous Level 1 is formed by slightly clayey sandy silts, lacking lamination.

140 Moleto 2 is 2.5 m wide and 0.4 to 0.5 m thick (Fig. 1D). The fissure is infilled by a
141 yellow ochraceous sandy clay sediment with scarce small and large vertebrate remains.

142 **3. Material and methods**

143 *3.1. Vertebrate sorting and taxonomic study*

144 The large mammal specimens and most of the small vertebrate material documented
145 herein were collected from the Moletto site during the 2009 sampling campaign conducted
146 by the Università degli Studi di Torino, in addition to the material recovered during a
147 survey carried out in Moletto 0 in the 1990s. Raw sediment retrieved on site in Moletto 1
148 and 2 was systematically water-screened using superimposed 2 and 0.8 mm mesh sieves.
149 The 0.8 mm mesh sieve was not used during the screening of the Moletto 0 sediment,
150 leading to a bias in the smaller specimens, as is the case for murids and *Muscardinus*,
151 groups expected to occur but apparently absent. The resulting Moletto small vertebrate
152 collection includes 209 identified small mammal teeth, mandibles, and maxillae (plus two
153 humeri of a talpid) corresponding to 13 different taxa, and 167 disarticulated cranial and
154 postcranial bones of amphibians and squamate reptiles comprising at least 8 taxa. 14 large
155 mammal teeth and bones belonging to eight taxa have also been recovered, together with
156 two avian bones representing a single taxon (see supplementary material 2). These fossils
157 are part of the collections of the Museo di Geologia e Paleontologia, Università degli
158 Studi di Torino (MGPT-PU) and are housed at the Dipartimento di Scienze della Terra,
159 Università degli Studi di Torino (Torino, Italy).

160 All the measurements are expressed in millimetres and were taken with the software
161 DinoCapture 2.0, using photographs from the Digital Microscope AM4115TL Dino-Lite
162 Edge. Small vertebrate remains are illustrated by means of digital photographs taken with
163 the same device. The upper teeth are marked with capital letters and the lower teeth by
164 lowercase letters. Taxonomy follows Speybroeck et al. (2020) for herpetofaunal taxa.
165 Osteological terminology follows Macaluso et al. (2023) for urodeles; Sanchiz (1998),
166 Bailon (1999), and Gómez and Turazzini (2016) for anurans; Villa and Delfino (2019)
167 and Čerňanský et al. (2019) for lizards; and Szyndlar (1984) for snakes. The terminology
168 and measuring methods employed in the descriptions of the arvicolid teeth (only m1 have

169 been considered) are those of Van der Meulen (1973), modified by Petruso et al. (2011)
170 for *Microtus (Terricola)*, and by Nadachowski (1984) and Cuenca-Bescós and Laplana
171 (1995) for *Microtus gr. arvalis-agrestis*. For *Arvicola*, we have calculated the SDQ index
172 (enamel differentiation index; Heinrich, 1978), which quantifies the difference in enamel
173 thickness between the anterior and the posterior wall of each triangle of arvicolid molars.
174 The index was calculated using complete m1 samples (SDQ7) following the formula:
175 $SDQ = [\sum (teet \times 100/leet)] / N$, where N is the number of dentine fields of the studied
176 tooth, teet (trailing edge enamel thickness) refers to the maximum thickness of the
177 posterior enamel band, and leet (leading edge enamel thickness) is the maximum
178 thickness of the anterior enamel band of each dentine field (Heinrich, 1978, 1987; von
179 Koenigswald and van Kolfschoten, 1996; Cuenca-Bescós et al., 2010; Lozano-Fernández
180 et al., 2013). In describing and measuring the glirid teeth, we have followed the
181 nomenclature and methods proposed by Daams (1981) and Freudenthal (2004),
182 respectively. Van de Weerd (1976) was followed when we describe murid teeth, and
183 length and width have been measured as defined by Martín-Suárez and Freudenthal
184 (1993). For the nomenclature and measurements of sciurids, we have followed Sinitsa
185 and Pogodina (2019) and Van de Weerd (1976), respectively. The terminology and
186 measurements used to describe lagomorphs remains follow Angelone and Sesé (2009).
187 We used the terminology and methods of Furió et al. (2015) for the Erinaceidae, of
188 Reumer (1984) for the Soricidae family, and of Hutchison (1974) for the Talpidae.

189 3.2. *Palaeoclimatic reconstructions*

190 Palaeoclimatic reconstructions were carried out following the Bioclimatic Model
191 (BM) on small mammal assemblages, and the Quantified Ecology (QE) and Mutual
192 Ecogeographic Range (MER) on the herpetofaunal assemblages.

193 The qualitative Bioclimatic Method was established by Hernández-Fernández
194 (2001a, 2001b) and updated by Royer et al. (2020). This analysis is based on the
195 hypothesis of a significant correlation between climate and mammal community
196 composition, applying multivariate discriminant analysis to modern mammal faunas and
197 climates throughout the world (Hernández-Fernández and Peláez-Campomanes, 2003).
198 The approach to the past climatic conditions at Moleto was based on the bioclimatic
199 components from the rodent and insectivore fauna (Hernández-Fernández and Peláez-
200 Campomanes, 2005; Royer et al., 2020). The bioclimatic characterisation of the living
201 and extinct species from Moleto that was required for calculation of the bioclimatic
202 spectra was taken from Hernández-Fernández (2001a, 2001b) and Hernández-Fernández
203 et al. (2007). According to this method, mammal assemblages can be assigned to ten
204 climate types, five of which are represented by the rodent assemblage in Moleto: IV -
205 subtropical with winter rains and summer droughts, VI - typical temperate, VII - arid
206 temperate, VIII - cold-temperate (boreal), and IX - polar. After obtaining this distribution,
207 we calculated the Bioclimatic Component, from which a mathematical model was
208 elaborated using a multiple linear regression (Hernández-Fernández and Peláez-
209 Campomanes, 2005). By means of a series of functions, this allows the estimation of
210 various climatic parameters, such as mean annual temperature (MAT) and mean annual
211 precipitation (MAP).

212 The Quantified Ecology method (Jeannet, 2010, 2018) is based on assigning
213 climato-ecological values, stemming from randomly collected geographic and climatic
214 data provided by remote climatic stations over 30 years, to each species in relation to their
215 climatic and ecological potentialities (Jeannet, 2010). For each species, the climatic data
216 provided by remote stations and averages thereof are associated with those of other
217 species of the same level. The values obtained for each parameter are given in Jeannet

218 (2010). The mean of all the species represented in a site and/or a level permits estimation
219 of various climatic parameters, such as the MAT, MAP, mean temperature of the warmest
220 month (MTW), and mean temperature of the coldest month (MTC). In cases of higher
221 taxa categories, the mean between the climate parameters of the different referred species
222 has been done. However, the somewhat important differences observed between the
223 weighting (according to Jeannet, 2010) of *Rana dalmatina* vs. *Rana temporaria*
224 concerning temperature (with the exception of MTW) and % of forested areas and of
225 *Natrix* gr. *natrix* vs. *Natrix tessellata* concerning temperature, rainfall, and % of forested
226 areas prevented proposal of any reasonable mean and have been disregarded here.

227 The Mutual Ecogeographic Range method (MER; Blain et al., 2009, 2016) was
228 used to identify the common current geographical range of the extant herpetofaunal
229 species present in the studied levels. The MER method is based on presence/absence (and
230 not abundance) and therefore is not particularly affected by taphonomic biases and/or
231 over-representation of some species in the fossil sites (Blain et al., 2016). This method
232 assumes that each species' and genus' ecological niche is preserved, so that extinct
233 populations of extant species have the same climatic tolerances and preferences as their
234 living representatives (Jackson and Overpeck, 2000; Jackson and Williams, 2004). To
235 determine the current spatial distributions of European amphibians and reptiles, we used
236 the data from Sillero et al. (2014) represented in a geographic coordinate system (datum
237 WGS 84) with a 50 × 50 km grid. In the cases where species-level identification was not
238 achieved (i.e. *Rana* sp. and *Vipera* gr. *aspis*), all the extant species belonging to the genus
239 or taxonomical group were taken into consideration (see Table S1 in supplementary
240 material 3). Once the common overlapping areas of the species from the assemblages
241 were obtained, in order to achieve a more precise common species distribution areas, the
242 fundamentals of the UDA-ODA discrimination technique were applied (Fagoaga et al.,

243 2019a; Marquina-Blasco et al., 2022). This recent procedure, partially derived from the
244 MER method, identifies the Occupied Distribution Area (ODA), which denotes realistic
245 occupied areas where the species may be present, and the UDA (Uncertain Distribution
246 Area) where the species may be absent. The technique sharpens each species distribution
247 using the species environmental requirements, creating the real ODA that were used to
248 determine the current analogue association from where climatic parameters will be
249 extrapolated to past fossil assemblages. In this case, the upper elevation limit has been
250 used to obtain more precise areas within the overlapping area in which all the species of
251 the three intersections analysed could coincide. The upper limit of elevation at which all
252 species in the assemblages could coincide has been established at 2000 m (based on
253 *Hierophis viridiflavus*; Vogrin et al., 2009).

254 Annual (MAT, MAP) and monthly climatic parameters (MTW, MTC) were
255 extracted from the final overlapping areas from climate layers belonging to WorldClim
256 2.1 with a 30 arcseconds resolution grid (Fick and Hijmans 2017). The same climatic
257 parameters were calculated for the recent vicinity of Ottiglio (1970–2001, with a 154 km²
258 area). Data sets were processed using the ArcGIS 10.3 application (ESRI 2014). The
259 mean and standard deviation were calculated using the statistical program IBM SPSS
260 Statistics 22 (IBM Corp. Released 2013).

261 3.3. *Palaeoenvironmental reconstruction*

262 In order to reconstruct the ecological conditions that prevailed in the area of Moletto
263 during the late Middle Pleistocene, we used the method of Habitat Weightings on small
264 mammals and herpetofauna (Evans et al., 1981; Andrews, 2006) and the Quantified
265 Ecology and MER methods on herpetofauna. These methods have not been applied to
266 large mammals and birds due to scarcity of material.

267 The Habitat Weightings method is based on the distribution of each small vertebrate
268 taxon in the habitat(s) where they are found today (for extant species) or where they are
269 assumed to have lived in the past (for extinct species). Habitats are divided into six types:
270 open dry meadows, open humid meadows, rocky areas, open woodland, woodland and
271 woodland-margin areas, and areas surrounding water (Cuenca-Bescós et al., 2005, 2009;
272 Blain et al., 2008; López-García et al., 2010, 2014; Piñero et al., 2016). Each taxon was
273 rated to a maximum score of 1.00, which was divided proportionally to its habitat
274 preferences if the species dwelled in more than one habitat type. To implement the Habitat
275 Weightings method, it was necessary to calculate the proportions of each taxon in the
276 assemblage using the minimum number of individuals (MNI).

277 In addition to the climatic parameters, Jeannet (2010) proposed some quantification
278 for environmental parameters. The Quantified Ecology method avoids the use of the MNI,
279 as it is judged to not always be representative of the environment (Jeannet, 2010). It thus
280 proposes to weight the preference of each species for forested environments, with mean
281 values representing a proxy for the extension of wooded (% of forested) environments
282 around the archaeo-palaeontological localities.

283 **4. Faunal content**

284 The vertebrate assemblage from Moleto includes up to 30 different taxa (see Table
285 1). Amphibians are represented by *Salamandra salamandra*, *Bufo* gr. *bufo*, and *Rana* sp.;
286 squamate reptiles by *Anguis* gr. *fragilis*, Lacertidae indet., *Hierophis* sp., *Natrix* sp., and
287 *Vipera* gr. *aspis* (Fig. 2). Among birds, only Passeriformes indet. has been identified (Fig.
288 2D). The small mammal association comprises *Erinaceus europaeus*, *Talpa europaea*,
289 *Sorex* sp., *Arvicola mosbachensis*, *Microtus (Terricola)* gr. *multiplex-subterraneus*,
290 *Microtus (Agricola)* cf. *agrestis*, *Microtus (Microtus)* cf. *arvalis*, *Apodemus* gr.

291 *sylvaticus-flavicollis*, *Sciurus* sp., *Glis glis*, *Muscardinus avellanarius*, *Clethrionomys*
292 *glareolus*, and Lagomorpha indet. (Fig. 3). The large mammal association includes
293 *Mustela putorius*, Carnivora indet., *Stephanorhinus* sp., *Sus* cf. *scrofa*, *Dama* cf. *dama*,
294 *Cervus elaphus*, *Capreolus capreolus*, Bovidae indet. (Fig. 4). Detailed taxonomic
295 descriptions and remarks for each taxon can be found in supplementary material 2. Tables
296 with measurements and additional digital photographs of rodent and insectivore remains
297 are provided in supplementary material 3.

298 **5. Remarks on the small mammal taphonomy**

299 The study of small mammal taphonomy employs a descriptive and systematic
300 approach, analysing alterations resulting from predation (Andrews, 1990; Fernandez-
301 Jalvo et al., 2016). In this preliminary study, we specifically observed and described the
302 modifications caused by digestion in the first lower molars of arvicoline rodent species,
303 as stated in Andrews (1990) and Fernandez-Jalvo et al. (2016). This enables us to
304 recognise the action of predators responsible for the accumulation of small mammal
305 remains.

306 Among the 49 analysed molars, 39% show evidence of light digestion,
307 characterised by the progressive reduction of enamel on the teeth. This suggests the
308 involvement of predators in the accumulations. The limited remains recovered from
309 Moleto 2 (two m1s) does not allow for a taphonomic interpretation. In Moleto 0, 38% of
310 arvicoline first lower molars are affected by light digestion, while in Moleto 1, the
311 percentage of lightly digested molars reaches 46%. The relatively low degree of alteration
312 in the Moleto sample, detected in less than 50%, indicates that the agent responsible for
313 the accumulation is likely a strigiform, such as *Athene noctua* or *Strix aluco* (according
314 to Andrews, 1990; Fernandez-Jalvo et al. 2016). Most authors consider that small

315 mammal remains in karstic sites are accumulated by the action of nocturnal avian
316 predators through the rejection of pellets rich in skeletal material after digestion (Dauphin
317 et al., 1996; Saavedra and Simonetti, 1998; Terry, 2004; Piñero et al. 2016).

318 The material from Moleto does not reveal any discernible pattern of prey
319 consumption, as described by Andrews (1990) and Fernandez-Jalvo et al. (2016).
320 Consequently, the palaeoecological interpretations based on the relative abundances of
321 small mammal taxa reliably indicate the habitat where predators consumed their prey.

322 **6. Chronological remarks**

323 Based on the rodent assemblage it is possible to estimate the chronology of Moleto.
324 European Plio-Pleistocene deposits are usually rich in arvicolids (voles), rodents
325 particularly suited for the dating of continental sediments of this time interval. The high
326 evolutionary rates and rapid diversification of this successful group, its unusually
327 adequate fossil record, and its cosmopolitanism make it an excellent tool for
328 biochronological correlations (Maul et al., 1998; Maul and Markova, 2007; Piñero et al.,
329 2018, 2020, 2022; Piñero and Agustí, 2019; among others). The arvicolid assemblage
330 from Moleto includes *Clethrionomys glareolus*, *Microtus (Terricola) gr. multiplex-*
331 *subterraneus*, *Microtus (Microtus) cf. arvalis*, *Microtus (Agricola) cf. agrestis* and
332 *Arvicola mosbachensis*. Among them, *Arvicola mosbachensis* is the most significant
333 biochronological element.

334 The oldest specimens of the living *Clethrionomys glareolus* date back to the late
335 Biharian (late Early Pleistocene; Glazek et al., 1976). This species has been documented
336 from several Middle and Late Pleistocene sites, becoming dominant in small mammal
337 assemblages between the Late Pleistocene and the Holocene (Nadachowski, 1982, 1989;
338 Kowalski, 2001; Krokmal et al., 2022). The first occurrence of the extant *Microtus*

339 *arvalis* and *Microtus agrestis* is still under debate due to problems of identification of
340 both species. However, the earliest remains of *Microtus* gr. *arvalis-agrestis* (or *Microtus*
341 aff. *arvalis-agrestis*) date back to the Early-Middle Pleistocene boundary (Maul and
342 Markova, 2007). On the other hand, *Microtus (Terricola)* is strictly related to the
343 subgenus *Microtus (Allophaiomys)*, which originated at the end of the Early Pleistocene.
344 In Italy, the oldest records of *Microtus (Terricola)* sp. are found in early Toringian sites
345 (Kowalski, 2001).

346 The genus *Arvicola* is one of the best time markers for Middle and Late Pleistocene
347 assemblages (Socha, 2014). Changes in its enamel thickness are used to establish
348 chronological schemes. *Arvicola mosbachensis* (= *A. cantianus*) is considered the ancestor
349 of *Arvicola amphibius* (= *A. terrestris*) in the lineage *Mimomys savini*-*Arvicola*
350 *mosbachensis*-*Arvicola amphibius*. This lineage is based on the late Biharian-Toringian
351 small mammal biozones (Fejfar and Heinrich, 1988; Maul and Markova, 2007; Sala and
352 Masini, 2007; Berto et al., 2021). The transition between the early Toringian (Middle
353 Pleistocene) and the late Toringian small mammal age (Late Pleistocene) is marked by
354 the progressive replacement of *Arvicola mosbachensis* by *Arvicola amphibius* with
355 modern morphology (López-García et al., 2017). The distinction between these two
356 species is based on the SDQ index, with a threshold ascertained at 100 (Heinrich, 1978).

357 *Arvicola* members with SDQ index around 100 are characteristic of the Middle/Late
358 Pleistocene boundary in western Europe (Rekovets, 1990, 1994; Rekovets and
359 Nadachowski, 1995; Markova, 2004, 2006). A pattern of progressive decline over time
360 in this index has been recognised (Berto et al., 2021). While *Arvicola* representatives with
361 SDQ exceeding 100 are generally considered to be characteristic of the Middle
362 Pleistocene, values close to or smaller than 100 are typical of the Late Pleistocene (Socha,
363 2014, and references therein). It should be noted that when samples from different

364 geographical areas are compared in detail, regional variations of SDQ values may be
365 observed. Such is the case for Italian water voles and their Central European counterparts,
366 but these variations are more evident in *A. amphibius* since the beginning of the Late
367 Pleistocene, while the *A. mosbachensis* of northern Italy presents the same characteristic
368 as the Central European ones (Masini et al. 2020).

369 The transition between *A. mosbachensis* and *A. amphibius* is not abrupt, having
370 been affected by morphological and geographical variability (Maul et al., 1998; Masini
371 et al., 2003; Paunescu et al., 2004). However, the first appearance of *A. amphibius* in Italy
372 precedes the end of the Eemian interglacial, MIS 5e (Sala and Masini, 2007; López-
373 García et al., 2017). In Moletto, all the SDQ values of *Arvicola* exceeds 100 (see Table S2
374 in supplementary material 3). These results suggest that the deposition of the three
375 fissures took place during the latest Middle Pleistocene (older than the Eemian
376 interglacial), when the mean SDQ values exceed 100, being within the range of variation
377 of SDQ for European representatives of *Arvicola* of that period (Fig. 5) (von
378 Koenigswald, 1973, 1980; Heinrich, 1978, 1982, 1987, 1990; van Kolfschoten, 1990;
379 Rekovets and Nadachowski, 1995; von Koenigswald and van Kolfschoten, 1996;
380 Desclaux et al., 2000; Maul et al., 2000; Kalthoff et al., 2007; Nadachowski et al., 2009;
381 Socha, 2014; Valde-Nowak and Nadachowski, 2014; Berto et al., 2021).

382 The Late Pleistocene site of De Nadale Cave (northeastern Italy), correlated to near
383 the onset of MIS 4 (71–57 ka), has some elements in common with Moletto such as
384 *Microtus (Terricola) multiplex-subterraneus*, *Clethrionomys glareolus*, *Microtus arvalis*,
385 *Microtus agrestis*, and *Apodemus gr. sylvaticus-flavicollis* (López-García et al., 2018).
386 However, De Nadale Cave includes *Arvicola amphibius*, descendant of *Arvicola*
387 *mosbachensis*, suggesting a younger age than Moletto. Similarly, the Late Pleistocene
388 sequence of Fumane Cave (MIS 3 to MIS 2), in northeastern Italy, shares with Moletto

389 the presence of the rodents *Microtus (Terricola) multiplex-subterraneus*, *Clethrionomys*
390 *glareolus*, *Microtus arvalis*, *Microtus agrestis*, *Apodemus* gr. *sylvaticus-flavicollis*, *Glis*
391 *glis*, and *Muscardinus avellanarius* (López-García et al., 2015). Nevertheless, the
392 occurrence of *Arvicola amphibius* in Fumane Cave indicates that Moletto is somewhat
393 older. This is also the case for the MIS 5 layers of Caverna degli Orsi (northeastern Italy;
394 Berto and Rubinato, 2013), and the MIS 5 locality of Ciota Ciara (Piedmont region; Berto
395 et al., 2016), which record some species also found in Moletto, but they include *Arvicola*
396 *amphibious* or *A. cf. amphibious* with SDQ values lower than those of Moletto, suggesting
397 a somewhat younger age than the studied site.

398 The rodent assemblage from the lower levels of Grotta Maggiore di San Bernardino
399 (northeastern Italy), dated to MIS 7 (López-García et al., 2017), is very similar to that of
400 Moletto. Similar taxa have been recognised in units VIII-VII such as *Arvicola*
401 *mosbachensis*, *Microtus (Terricola) multiplex-subterraneus*, *Clethrionomys glareolus*,
402 *Microtus arvalis*, *Microtus agrestis*, and *Apodemus* gr. *sylvaticus-flavicollis*, *Sciurus* sp.,
403 and *Glis glis*, suggesting that they have a very close age (Fig. 6). The younger units IV-
404 V (MIS 5) and III-II (MIS 3) already include a modern form of *Arvicola* (*A. amphibius*).

405 According to all of these evidences, the assemblages from Moletto likely date back
406 to the late Middle Pleistocene, older than MIS 5e (MIS 8–6, probably interglacial MIS 7
407 as discussed in the next section). However, we cannot exclude that Moletto 0, 1, and 2
408 were deposited at the boundary of the Middle and Late Pleistocene. Although the SDQ
409 values for all deposits exceeded 100, the paucity of data makes it difficult to interpret the
410 results unambiguously.

411 **7. Environmental approach**

412 Small mammals, amphibians, and reptiles have been widely used as palaeoclimatic
413 and palaeoecological indicators, allowing to reconstruct past environmental and climatic
414 conditions (e.g. Blain et al., 2009; Piñero et al., 2016; Lozano-Fernández et al., 2019;
415 López-García et al., 2021; Sánchez-Bandera et al., 2023). Here, we attempt to analyse the
416 environment and climate in the area of Moletto at the time of the deposition of the
417 fossiliferous sediments.

418 The Habitat Weightings method applied to the small mammal assemblage of the
419 Moletto site reveals an environment dominated by woodland and open woodland habitats
420 (66.7%), represented mainly by the species *Glis glis*, *Apodemus* gr. *sylvaticus-flavicollis*,
421 and *Clethrionomys glareolus*. There was also an important presence of water streams
422 (8.3%) and open humid meadows (18.8%), indicated by the relative abundance of
423 *Arvicola mosbachensis* and *Microtus (Terricola)* gr. *multiplex-subterraneus* (Table 2).
424 The presence of open dry areas was limited to 6.3%.

425 The results obtained from the Habitat Weightings method using the amphibian and
426 squamate reptile assemblages (Table 2) again suggest the dominance of woodland and
427 open woodland areas (48.6%), with presence of water streams (10.7%), and a high
428 representation of open moist areas (33.6%). Open dry meadows are poorly represented
429 (7.1%). The percentage of forest is somewhat higher in data provided by the small
430 mammal assemblage, but the overall palaeoenvironmental results are very close. It is
431 usual that reconstructions based exclusively on small mammals (e.g. Fagoaga et al.,
432 2019b) provide higher forest values than those based on herpetofauna (Marquina-Blasco
433 et al., 2017, 2021).

434 The percentage of wooded areas obtained with the small mammal assemblage
435 agrees well with the palaeoenvironmental results obtained from Quantified Ecology
436 (Jeannet, 2010) on the amphibian and squamate reptile assemblages from Moletto, which

437 indicate 64% of forest cover (Table 3). Similarly, according to the data obtained from
438 Mutual Ecogeographic Range, the extension of wooded environments in Moledo reached
439 51.8%, 7% higher than that of today.

440 Overall, the small mammal and herpetofaunal assemblages suggest the prevalence
441 of a landscape dominated mainly by woodland and open-woodland areas, with presence
442 of open herbaceous areas and development of water courses in the vicinity of Moledo
443 during the formation of the site (Fig. 7). The predominance of forested environments at
444 Moledo is supported by the appearance of browsing herbivores, such as the red deer
445 (*Cervus elaphus*), roe deer (*Capreolus capreolus*), and fallow deer (*Dama dama*). In
446 addition, the preferred habitats by wild boars (*Sus scrofa*) and European polecats (*Mustela*
447 *putorius*), present at Moledo, are mixed forests under humid conditions (Petronio et al.,
448 2011). The existence of open environments and open woodlands around Moledo is
449 consistent with the occurrence of a large bovid (such as *Bison* or *Bos*) and the rhinoceros
450 *Stephanorhinus* sp. (Petronio et al., 2011).

451 **8. Palaeoclimatic reconstruction**

452 The present-day climate in Moledo is characterized by a mean annual precipitation
453 (MAP) of 1137 mm, and a mean annual temperature (MAT) of 12.7 °C. The thermal
454 gradient ranges approximately from 23.8 °C (mean temperature of warmest month,
455 MTW) to 1.7 °C (mean temperature of coldest month, MTC) (Climate-data.org).

456 The palaeoclimatic results obtained from Quantified Ecology (Jeannet, 2010)
457 applied to the herpetofaunal assemblages (Table 4) point to a slightly cooler climate with
458 relatively lower rainfall than today (Fig. 7). The MAT was 2.3 °C lower, and the MAP
459 402 mm lower than present-day values. The MTC was 1 °C, and the MTW was 20.8 °C,
460 a thermal gradient close to the current one. Likewise, the results attained from Mutual

461 Ecogeographic Range (MER) using UDA/ODA technique on the herpetofauna
462 assemblages (Table 5; Fig. S6) suggest somewhat colder temperatures than today (MAT
463 = 10.7 °C, MTC = 2.4 °C, MTW = 19 °C). The MER reconstructed rainfall suggests,
464 however, MAP closer to current data (MAP = 880 mm).

465 The data obtained by the Bioclimatic Model (BM) on small mammals suggest MAT
466 2.8 °C lower than nowadays in the area of Moletto, but standard deviation with ± 6.9 °C
467 overlaps with the current ones. Similar to the herpetofaunal assemblages, the small
468 mammals from Moletto suggests mild summers, with $MTW = 20.8 \pm 5.5$ °C, and relatively
469 cold winters, with $MTC = -0.8 \pm 15.9$ °C. This thermal gradient is similar to the current
470 one in the area (Table 6). The BM reconstructed rainfall also indicates a drier climate
471 ($\Delta MAP = -551.1$ mm) (Fig. 7). The bioclimatic components are dominated by the climate
472 VI (43%) (typical temperate, related with a temperate deciduous forest), indicating winter
473 rain and summer drought. It is followed by climate VIII (23.6%) (cold-temperate, related
474 to a boreal coniferous forest-taiga), denoting cold-temperate conditions (Royer et al.,
475 2020) (Table 7).

476 The climatic parameters reconstructed using the herpetofauna and those
477 reconstructed with small mammals are coherent (Fig. 7). The results of all the
478 palaeoclimate methods suggest that the small vertebrate assemblage from Moletto was
479 probably related to temperate and moist climatic conditions. This is consistent with
480 deposition during an interglacial event, thus discarding the late Middle Pleistocene cold
481 MIS 8 and MIS 6 periods.

482 When comparing the palaeoclimatic data of Moletto with those of the nearby MIS 6
483 site of Lazaret (Nice, France) (López-García et al., 2021), located around 160 km
484 southwest of Moletto, we observe that the MAT reconstructed at Lazaret (~ 8.8 °C) is lower
485 than that of Moletto (~ 10 °C). Most remarkable is the marked contrast between the current

486 MAT at Nice (15 °C) and that of Lazaret ($\Delta\text{MAT} = -6.2$ °C), representing a significantly
487 more pronounced difference than in Moletto (<3 °C). In addition, the percentage of forest
488 at Lazaret cave (ca. 35%) is lower than that of Moletto. These data support the dismissal
489 of the correlation of Moletto with the glacial MIS 6.

490 According to the chronological data presented above, the interglacial stage of
491 Moletto would correspond to MIS 7. Considering that the reconstructed MAT is somewhat
492 cooler than today, Moletto may have been deposited during a cold episode within MIS 7
493 such as MIS 7d (the cold substage 7b is less severe). Alternatively, the site could represent
494 a transition between MIS 7 and MIS 6 (Fig. 7). Nevertheless, more solid chronological
495 data are essential to reach a firm conclusion on this regard.

496 Studies of small vertebrates from late Middle Pleistocene sites in Italy are limited.
497 Three of these sites are Torre in Pietra 2 (Latium) (Caloi and Palombo, 1978), Sossano 2
498 (Berici Hills, Vicenza) (Bon et al., 1991), and lower units (VIII-VII) of Grotta Maggiore
499 di San Bernardino (Berici Hills, Vicenza) (López-García et al., 2017). Among them, only
500 Grotta Maggiore di San Bernardino has a palaeoenvironmental and palaeoclimatic study
501 comparable to that of Moletto. According to López-García et al. (2017, 2019), the lower
502 units of the nearby Grotta Maggiore di San Bernardino site are characterized by the
503 dominance of forest species such as *A. gr. Sylvaticus-flavicollis*, *G. glis*, and *C. glareolus*.
504 The presence of water streams (mainly suggested by the abundance of *A. mosbachensis*)
505 and open humid meadows (indicated by the relative abundance of *M. agrestis* or *Talpa*
506 *cf. europaea*) is also important in units VIII-VII of Grotta Maggiore di San Bernardino.
507 Thus, as in Moletto, these MIS 7 levels are characterized by the predominance of
508 woodland formations and temperate and moist climatic conditions (López-García et al.,
509 2017, 2019).

510 **9. Conclusions**

511 The vertebrate assemblage from Moleto is represented by amphibians (*Salamandra*
512 *salamandra*, *Bufo* gr. *Bufo*, *Rana* sp.), squamate reptiles (*Anguis* gr. *Fragilis*, Lacertidae
513 indet., *Hierophis* sp., *Natrix* sp., *Vipera* gr. *Aspis*), birds (Passeriformes indet.), and
514 mammals (*Erinaceus europaeus*, *Talpa europaea*, *Sorex* sp., *Arvicola mosbachensis*,
515 *Microtus (Terricola)* gr. *Multiplex-subterraneus*, *Microtus (Agricola)* cf. *agrestis*,
516 *Microtus (Microtus)* cf. *arvalis*, *Clethrionomys glareolus*, *Apodemus* gr. *Sylvaticus-*
517 *flavicollis*, *Sciurus* sp., *Glis glis*, *Muscardinus avellanarius*, Lagomorpha indet., *Mustela*
518 *putorius*, Carnivora indet., *Stephanorhinus* sp., *Sus* cf. *scrofa*, *Dama* cf. *dama*, *Cervus*
519 *elaphus*, *Capreolus capreolus*, Bovidae indet.). The overall assemblage composition is
520 typical of a warm phase and such elements are not present in assemblages dated later than
521 MIS 5. The enamel characteristics of the rodent *Arvicola mosbachensis* indicates a latest
522 Middle Pleistocene age. A multi-method approach using the small mammal and
523 herpetofaunal assemblages point to the dominance of forested environments in Moleto
524 during the deposition of the site, with development of open grassy areas and water
525 courses. The palaeoclimatic data suggest temperate and moist climatic conditions, with
526 slightly cooler temperatures and lower rainfall than today. According to the age of the
527 site and palaeoclimatic results, the accumulation of remains may have occurred during
528 the interglacial MIS 7. The Moleto site thus joins other European localities from the latest
529 Middle Pleistocene, contributing to improve the knowledge of vertebrate communities,
530 climate and environment in northern Italy during the Middle–Late Pleistocene boundary.

531 **Declaration of competing interest**

532 The authors declare that they have no known competing financial interests or
533 personal relationships that could have appeared to influence the work reported in this
534 paper.

535 **Acknowledgements**

536 This work was supported by the Spanish Ministry of Science and Innovation
537 (MCIN/AEI/10.13039/501100011033/FEDER ‘Una manera de hacer Europa’) [grant
538 numbers I+D+i PID2020-117289GBI00, PID2021-123092NB-C21, and PID2021-
539 122533NB-100]; AGAUR-Generalitat de Catalunya [grant numbers 2021 SGR 00620
540 and 2021SGR-01238]; Universitat Rovira i Virgili [grant number 2023PFR-URV-
541 01238]; and Fondi di Ricerca Locale, Università di Torino (2019–2022). The research of
542 PP, JMLG, H-AB, CSB, and AV is funded by the CERCA Programme/Generalitat de
543 Catalunya. PP is supported by a “Juan de la Cierva-Incorporación” contract [grant
544 IJC2020-044108-I] funded by MCIN/AEI/10.13039/501100011033 and “European
545 Union NextGenerationEU/PRTR”. MF is a Serra Húnter Fellow. AV is supported by the
546 Secretaria d'Universitats i Recerca of the Departament de Recerca i Universitats,
547 Generalitat de Catalunya, through a Beatriu de Pinós postdoctoral grant (2021 BP 00038).
548 CSB is supported by a FPI Predoctoral Scholarship [grant PRE2020-094482] associated
549 with project funded by the Spanish Ministry of Science and Innovation [grant CEZ2019-
550 000945-M-20-1]. PP, JMLG, H-AB, and CSB belong to the Consolidated Research
551 Group “Paleoecology of Pliocene and Pleistocene and Human Dispersals (PalHum)”. The
552 Institut Català de Paleoecologia Humana I Evolució Social (IPHES-CERCA) received
553 financial support from the Spanish Ministry of Science and Innovation through the “María
554 de Maeztu” programme for Units of Excellence [CEX2019-000945-M]. The research of
555 GC, LM, GM, GP, MP, and MD was supported by grants (ex-60% 2022 and 2023) from
556 the Università degli Studi di Torino. We thank Drs Chiara Angelone and Jordi Agustí for
557 providing helpful suggestions for the remarks on lagomorphs and glirids, respectively.
558 We would like to thank the two anonymous reviewers and the guest editor Iván Rey
559 Rodríguez for their constructive comments on an earlier version of the manuscript. This

560 is the publication number XXX of the Museo di Geologia e Paleontologia collections at
561 the Università degli Studi di Torino.

562 **Appendix A. Supplementary data**

563 Supplementary data to this article can be found online at <https://doi.org/xxxxx>

564 **References**

565 Andrews, P., 1990. Owl, Caves and Fossils. Natural History Museum Publications,
566 London, pp. 1–231.

567 Andrews, P., 2006. Taphonomic effects of faunal impoverishment and faunal mixing.
568 *Palaeogeogr. Palaeoclimatol. Palaeoecol.* 241, 572–589.

569 Angelone, C., Sesé, C., 2009. New characters for species discrimination within the genus
570 *Prolagus* (Ochotonidae, lagomorpha, mammalia). *J. Paleontol.* 83, 80–88.

571 Bailon, S., 1999. Différenciation ostéologique des anoures (Amphibia, Anura) de France,
572 in: Desse, J., Desse-Berset, N. (Eds.), *Fiches d'ostéologie animale pour l'Archéologie*,
573 *Série C. APDCA, Antibes*, pp. 1–41.

574 Bartolomei, G., 1980. Micromammiferi del Plio-Pleistocene, in: Cigala Fulgosi, F.,
575 Kotsakis, T., Massari, F., Sorbini, L. (Eds.), *I Vertebrati Fossili Italiani, Catalogo Della*
576 *Mostra. Museo Civico di Storia Naturale di Verona, Verona*, pp. 249–258.

577 Benvenuti, M., Bahain, J.J., Capalbo, C., Capretti, C., Ciani, F., D'Amico, C., Esu, D.,
578 Giachi, G., Giuliani, C., Gliozzi, E., Lazzeri, S., Macchioni, N., Lippi, M.M., Masini, F.,
579 Mazza, P.P., Pallecchi, P., Revedin, A., Savorelli, A., Spadi, M., Sozzi, L., Vietti, A.,
580 Voltaggio, M., Aranguren, B., 2017. Paleoenvironmental context of the early
581 Neanderthals of Poggetti Vecchi for the late middle Pleistocene of Central Italy. *Quat.*
582 *Res.* 88(2), 327–344.

583 Berto, C., Rubinato, G., 2013. The upper Pleistocene mammal record from Caverna degli
584 Orsi (San Dorligo della Valle-Dolina, Trieste, Italy): a faunal complex between eastern
585 and western Europe. *Quat. Int.* 284, 7–14.

586 Berto, C., Berté, D., Luzi, E., López-García, J.M., Pereswiet-Soltan, A., Arzarello, M.,
587 2016. Small and large mammals from the Ciota Ciara cave (Borgosesia, Vercelli, Italy):
588 an isotope stage 5 assemblage. *C. R. Palevol* 15, 669–680.

589 Berto, C., Boscato, P., Boschin, F., Luzi, E., Ronchitelli, A., 2017. Paleoenvironmental
590 and paleoclimatic context during the Upper Palaeolithic (late Upper Pleistocene) in the
591 Italian Peninsula. The small mammal record from Grotta Paglicci (Rignano Garganico,
592 Foggia, Southern Italy). *Quat. Sci. Rev.* 168, 30–41.

593 Berto, C., López-García, J.M., Luzi, E., 2019. Changes in the Late Pleistocene small-
594 mammal distribution in the Italian Peninsula. *Quat. Sci. Rev.* 225, 106019.

595 Berto, C., Nadachowski, A., Pereswiet-Soltan, A., Lemanik, A., Kot, M., 2021. The
596 Middle Pleistocene small mammals from the lower layers of Tunel Wielki Cave (Kraków-
597 Częstochowa Upland): An Early Toringian assemblage in Poland. *Quat. Int.* 577, 52–70.

598 Blain, H.-A., Bailon, S., Cuenca-Bescós, G., 2008. The Early–Middle Pleistocene
599 palaeoenvironmental change based on the squamate reptile and amphibian proxies at the
600 Gran Dolina site, Atapuerca, Spain. *Palaeogeogr. Palaeoclimatol. Palaeoecol.* 261, 177–
601 192.

602 Blain, H.-A., Bailon, S., Cuenca-Bescós, G., Arsuaga, J.L., Bermúdez de Castro, J.M.,
603 Carbonell, E., 2009. Long-term climate record inferred from Early-Middle Pleistocene
604 amphibian and squamate reptile assemblages at the Gran Dolina cave, Atapuerca, Spain.
605 *J. Hum. Evol.* 56, 55–65.

606 Blain, H.-A., Lozano-Fernández, I., Agustí, J., Bailon, S., Menéndez Granda, L.,
607 Espígares-Ortiz, M.P., Ros-Montoya, S., Jiménez-Arenas, J.M., Toro-Moyano, I.,
608 Martínez-Navarro, B., 2016. Refining upon the climatic background of the Early
609 Pleistocene hominid settlement in Western Europe: barranco León and Fuente Nueva-3
610 (Guadix-Baza Basin, SE Spain). *Quat. Sci. Rev.* 144, 132–144.

611 Blain, H.-A., Rubio-Jara, S., Panera, J., Uribebarrea, D., Laplana, C., Herráez, E., Pérez-
612 González, A., 2017. A new middle Pleistocene (marine oxygen isotope stage 6) cold
613 herpetofaunal assemblage from the central Iberian Peninsula (Manzanares Valley,
614 Madrid). *Quat. Res.* 87, 499–515.

615 Bon, M., Piccoli, G., Sala, B., 1991. I giacimenti quaternari di vertebrati fossili nell'Italia
616 Nord-Orientale. *Mem. Sci. Geol.* 43, 185–231.

617 Bonsignore, G., Bortolami, G., Elter, G., Montrasio, A., Petrucci, F., Ragni, U., Sacchi,
618 R., Sturani, C., Zanella, E., 1969. Note illustrative dei Fogli 56–57, Torino-Vercelli della
619 Carta Geologica d'Italia alla scala 1:100.000. Ercolano, Poligrafica & Cartevalori, 96.

620 Caloi, L., Palombo, M.R., 1978. Anfibi, rettili e mammiferi di Torre del Pagliaccetto
621 (Torre in Pietra, Roma). *Quaternaria* 20, 315–428.

622 Čerňanský, A., Yaryhin, O., Ciceková, J., Werneburg, I., Hain, M., Klembara, J., 2019.
623 Vertebral comparative anatomy and morphological differences in anguine lizards with a
624 special reference to *Pseudopus apodus*. *Anat. Rec.* 302, 232–257.

625 Clari, P., Dela Pierre, F., Novaretti, A., Timpanelli, M., 1994. La successione oligo-
626 miocenica del Monferrato occidentale: confronti e relazioni con il Monferrato orientale e
627 la Collina di Torino. *Atti Tic. Sc. Terra, Ser. Spec.* 1, 191–203.

628 Colamussi, V., 2002. Studi climatici sul Quaternario mediante l'uso dei micromammiferi.
629 PhD Thesis, Università di Ferrara, Firenze, Parma.

630 Cuenca-Bescós, G., Laplana, C., 1995. Evolución de *Iberomys* (Arvicolidae, Rodentia,
631 Mammalia) durante el Cuaternario español, in: López, G., Obrador, A., Vicens, E. (Eds.),
632 XI Jornadas de Paleontología. Sociedad Española de Paleontología. Tremp, Lleida, pp.
633 69–72.

634 Cuenca-Bescós, G., Rofes, J., García Pimienta, J.C., 2005. Environmental change across
635 the early-middle Pleistocene transition: small mammalian evidence from the Trinchera
636 Dolina cave, Atapuerca, Spain, in: Head, M.J., Gibbard, P.L. (Eds.), Early Middle
637 Pleistocene Transitions: the Land-Ocean Evidence. Geological Society Special Issue,
638 London, pp. 27–38.

639 Cuenca-Bescós, G., Straus, L.G., González Morales, M., García Pimienta, J.C., 2009.
640 There construction of past environments through small mammals: from the Mousterian
641 to Bronze Age in El Mirón cave. *J. Archaeol. Sci.* 36, 947–955.

642 Cuenca-Bescós, G., Agustí, J., Lira, J., Rubio, M.M., Rofes, J., 2010. A new species of
643 water vole from the Early Pleistocene of Southern Europe. *Acta Palaeontol. Pol.* 55, 565–
644 580.

645 Daams, R., 1981. The dental pattern of the dormice *Dryomys*, *Myomimus*, *Microdyromys*
646 and *Peridyromys*. *Utrecht Micropaleontol. Bull.* 3, 1–115.

647 Dauphin, Y., Denys, C., Kowalski, K., Rzebik-Kowalska, B., 1996. Taphonomic study
648 of Algerian owl pellet assemblages and differential preservation of some rodents:
649 palaeontological implications. *Acta Zool. Cracov.* 39, 103–116.

650 Dennell, R.W., Martín-Torres, M., Bermúdez de Castro, J.M., 2011. Hominin
651 variability, climatic instability and population demography in Middle Pleistocene Europe.
652 Quat. Sci. Rev. 30, 1511–1524.

653 Desclaux, E., Abbassi, M., Marquet, J.-C., Chaline, J., van Kolfschoten, T., 2000.
654 Distribution and evolution of *Arvicola* Lacépède, 1779 (Mammalia, Rodentia) in France
655 and Liguria (Italy) during the Middle and the Upper Pleistocene. Acta Zool. Cracov. 43,
656 107–125.

657 Desprat, S., Goñi, M.F.S., Turon, J.L., Duprat, J., Malaizé, B., Peypouquet, J.P., 2006.
658 Climatic variability of Marine Isotope Stage 7: direct land-sea-ice correlation from a
659 multiproxy analysis of a north-western Iberian margin deep-sea core. Quat. Sci. Rev. 25,
660 1010–1026.

661 Ehlers, J., Grube, A., Stephan, H.-J., Wansa, S., 2011. Pleistocene glaciations of North
662 Germany—new results, in: Ehlers, J., Gibbard, P.L., Hughes, P.D. (Eds.), Quaternary
663 Glaciations - Extent and Chronology: A Closer Look. Developments in Quaternary
664 Sciences. Vol. 15. Elsevier, Amsterdam, pp. 149–162.

665 Evans, E.M.N., Van Couvering, J.A.H., Andrews, P., 1981. Palaeoecology of Miocene
666 sites in western Kenya. J. Hum. Evol. 10, 99–116.

667 Fagoaga, A., Blain, H.-A., Marquina-Blasco, R., Laplana, C., Sillero, N., Galván, B.,
668 Ruiz-Sánchez, F.J., 2019a. Improving the accuracy of small vertebrate-based
669 palaeoclimatic reconstructions derived from the Mutual Ecogeographic Range. A case
670 study using geographic information systems and UDA-ODA discrimination
671 methodology. Quat. Sci. Rev. 223, 105969.

672 Fagoaga, A., Laplana, C., Marquina-Blasco, R., Machado, J., Marin-Monfort, M.D.,
673 Crespo, V.D., Hernández, C.M., Mallol, C., Galván, B., Ruiz-Sánchez, F.J., 2019b.

674 Palaeoecological context for the extinction of the Neanderthals: a small mammal study
675 of stratigraphic Unit V of the El Salt site, Alcoi, eastern Spain. *Palaeogeogr.*
676 *Palaeoclimatol. Palaeoecol.* 530, 163–175.

677 Fejfar, O., Heinrich, W.-D., 1988. Muroid rodent biochronology of the Neogene and
678 Quaternary of Europe, in: Lindsay, E.H., Fahlbusch, V., Mein, P. (Eds.), *European*
679 *Neogene Mammal Chronology*. Springer Science & Business Media, pp. 91–117.

680 Fernández-Jalvo, Y., Andrews, P., Denys, C., Sesé, C., Stoetzel, E., Marin-Monfort, D.,
681 Pesquero, D., 2016. Taphonomy for taxonomists: implications of predation in small
682 mammal studies. *Quat. Sci. Rev.* 139, 138–157.

683 Fick, S.E., Hijmans, R.J., 2017. WorldClim 2: new 1-km spatial resolution climate
684 surfaces for global land areas. *Int. J. Climatol.* 37, 4302–4315.

685 Freudenthal, M., 2004. Gliridae (Rodentia, Mammalia) from the Eocene and Oligocene
686 of the Sierra Palomera (Teruel, Spain). *Treb. Mus. Geol. Barcelona* 12, 97–173.

687 Furió, M., Gibert, L., Ferràndez, C., Sevilla, P., 2015. The insectivores (Soricidae,
688 Erinaceidae; Eulipotyphla; Mammalia) from Cueva Victoria (Early Pleistocene, Murcia,
689 Spain). *Neues Jahrb. fur Geol. Palaontol.* 275, 151–161.

690 Głazek, J., Lindner, J., Wysoczański-Minkowicz, T., 1976. Interglacial Mindel I/Mindel
691 II in fossil-bearing karst at Kozi Grzbiet in the Holy Cross Mts. *Acta Geol. Pol.* 26, 377–
692 394.

693 Gómez, R.O., Turazzini G.F., 2016. An overview of the ilium of anurans (Lissamphibia,
694 Salientia), with a critical appraisal of the terminology and primary homology of main ilial
695 features. *J. Vertebr. Paleontol.* 36, e1030023.

696 Heinrich, W.D., 1978. Zur biometrischen erfassung eines evolutionstrends bei *Arvicola*
697 (Rodentia, Mammalia) aus dem Pleistozän Thüringens. Säugetierkd. Inform. 2/3, 3–21.

698 Heinrich, W.D., 1982. Zur Evolution und Biostratigraphie von *Arvicola* (Rodentia,
699 Mammalia) im Pleistozän Europas. Z. Geol. Wiss. 10, 683–735.

700 Heinrich, W.D., 1987. Neue Ergebnisse zur Evolution und Biostratigraphie von *Arvicola*
701 (Rodentia, Mammalia) im Quartär Europas. Z. Geol. Wiss. 15, 389–406.

702 Heinrich, W.D., 1990. Some aspects of the evolution and biostratigraphy of *Arvicola*
703 (Mammalia, Rodentia) in the Central European Pleistocene, in: Fejfar, O., Heinrich, W.-
704 D. (Eds.), International Symposium Evolution, Phylogeny and Biostratigraphy of
705 Arvicolids (Rodentia, Mammalia). Geological Survey, Prague, pp. 165–182.

706 Hernández-Fernández, M., 2001a. Bioclimatic discriminant capacity of terrestrial
707 mammal faunas. Glob. Ecol. Biogeogr. 10, 189–204.

708 Hernández-Fernández, M., 2001b. Análisis paleoecológico y paleoclimático de las
709 sucesiones de mamíferos del Plio-Pleistoceno ibérico. PhD Thesis, Universidad
710 Complutense de Madrid, Madrid.

711 Hernández-Fernández, M., Peláez-Campomanes, P., 2003. The bioclimatic model: a
712 method of palaeoclimatic qualitative inference based on mammal associations. Glob.
713 Ecol. Biogeogr. 12, 507–517.

714 Hernández-Fernández, M., Peláez-Campomanes, P., 2005. Quantitative palaeoclimatic
715 inference based on mammal faunas. Glob. Ecol. Biogeogr. 14, 39–56.

716 Hernández-Fernández, M., Álvarez-Sierra, M.A., Peláez-Campomanes, P., 2007.
717 Bioclimatic analysis of rodent palaeofaunas reveals severe climatic changes in

718 Southwestern Europe during the Plio-Pleistocene. *Palaeogeogr. Palaeoclimatol.*
719 *Palaeoecol.* 251, 500–526.

720 Hutchison, J.H., 1974. Notes on type specimens of European Miocene Talpidae and a
721 tentative classification of old world Tertiary Talpidae (Insectivora: Mammalia). *Geobios*
722 7, 211–256.

723 IBM Corp. Released. 2013. IBM SPSS Statistics for Windows, Version 22.0. Armonk
724 (NY), IBM Corp.

725 Jackson, S.T., Overpeck, J.T., 2000. Responses of plant populations and communities to
726 environmental changes of the late Quaternary. *Paleobiology* 26, 194–220.

727 Jackson, S.T., Williams, J.W., 2004. Modern analogs in Quaternary paleoecology: here
728 today, gone yesterday, gone tomorrow? *Annu. Rev. Earth Planet. Sci.* 32, 495–537.

729 Jeannet, M., 2010. L'écologie quantifiée. Essai de description de l'environnement
730 continental à l'aide des microvertébrés. *Préhistoires Méditerranéennes* 2010 (1), 1–26.

731 Jeannet, M., 2018. Vergisson II (Saône-et-Loire, France): microfauna and environment
732 of the man of Neanderthal. *Quaternaire* 29, 233–242.

733 Kalthoff, D.C., Mörs, T., Tesakov, A., 2007. Late Pleistocene small mammals from the
734 Wannenköpfe volcanoes (Neuwied Basin, western Germany) with remarks on the
735 stratigraphic range of *Arvicola terrestris*. *Geobios* 40, 609–623.

736 Krokmal, O., Rekovets, L., Kovalchuk, O., 2022. Biochronological scheme of the
737 Quaternary of the south of Eastern Europe and its substantiation based on arvicoline teeth
738 morphometrics. *Quat. Int.* <https://doi.org/10.1016/j.quaint.2022.12.003>

739 Kowalski, K., 2001. Pleistocene Rodents of Europe. *Folia Quat.* 72, 3–389.

740 Kukla, G.J., Bender, M.L., de Beaulieu, J.-L., Bond, G., Broecker, W.S., Cleveringa, P.,
741 Gavin, J.E., Herbet, T.D., Imbrie, J., Jouzel, J., Keigwin, L.D., Knudsen, K.-L.,
742 McManus, J.F., Merket, J., Muhs, D.R., Müller, H., Poore, R.Z., Porter, S.C., Seret, G.,
743 Shackleton, N.J., Turner, C., Tzedakis, P.C., Winograd, I.J., 2002. Last interglacial
744 climates. *Quat. Res.* 58, 2–13.

745 López-García, J.M., Blain, H.-A., Cuenca-Bescós, G., Ruiz-Zapata, M.B., Dorado-
746 Valiño, M., Gil-García, M.J., Valdeolmillos, A., Ortega, A.I., Carretero, J.M., Arsuaga,
747 J.L., Bermúdez de Castro, J.M., Carbonell, E., 2010. Palaeoenvironmental and
748 palaeoclimatic reconstruction of the latest Pleistocene of El Portalón site, Sierra de
749 Atapuerca, northwestern Spain. *Palaeogeogr. Palaeoclimatol. Palaeoecol.* 292, 453-464.

750 López-García, J.M., Berto, C., Colamussi, V., Dalla Valle, C., Lo Vetro, D., Luzi, E.,
751 Malavasi, G., Martini, F., Sala, B., 2014. Palaeoenvironmental and palaeoclimatic
752 reconstruction of the latest Pleistocene-Holocene sequence from Grotta del Romito
753 (Calabria, southern Italy) using the small-mammal assemblages. *Palaeogeogr.*
754 *Palaeoclimatol. Palaeoecol.* 409, 169–179.

755 López-García, J.M., Dalla Valle, C., Cremaschi, M., Peresani, M., 2015. Reconstruction
756 of the Neanderthal and Modern Human landscape and climate from the Fumane cave
757 sequence (Verona, Italy) using small-mammal assemblages. *Quat. Sci. Rev.* 128, 1–13.

758 López-García, J.M., Luzi, E., Peresani, M., 2017. Middle to Late Pleistocene
759 environmental and climatic reconstruction of the human occurrence at Grotta Maggiore
760 di San Bernardino (Vicenza, Italy) through the small-mammal assemblage. *Quat. Sci.*
761 *Rev.* 168, 42–54.

762 López-García, J.M., Livraghi, A., Romandini, M., Peresani, M., 2018. The De Nadale
763 Cave (Zovencedo, Berici Hills, northeastern Italy): A small-mammal fauna from near the

764 onset of Marine Isotope Stage 4 and its palaeoclimatic implications. *Palaeogeogr.*
765 *Palaeoclimatol. Palaeoecol.* 506, 196–201.

766 López-García, J.M., Berto, C., Peresani, M., 2019. Environmental and climatic context
767 of the hominin occurrence in northeastern Italy from the late Middle to Late Pleistocene
768 inferred from small-mammal assemblages. *Quat. Sci. Rev.* 216, 18–33.

769 López-García, J.M., Blain, H.-A., Sánchez-Bandera, C., Cohen, J., Lebreton, L.,
770 Montuire, S., Stewart, J.R., Desclaux, E., 2021. Multi-method approach using small
771 vertebrate assemblages to reconstruct the Marine Isotope Stage 6 climate and
772 environment of the Lazaret cave sequence (Maritime Alps, Nice, France). *Palaeogeogr.*
773 *Palaeoclimatol. Palaeoecol.* 577, 110529.

774 Lozano-Fernández, I., Agustí, J., Cuenca-Bescós, G., Blain, H.-A., López-García, J.M.,
775 Vallverdu, J., 2013. Pleistocene evolutionary trends in dental morphology of *Mimomys*
776 *savini* (Rodentia, Mammalia) from Iberian peninsula and discussion about the origin of
777 the genus *Arvicola*. *Quaternaire* 24, 179–190.

778 Lozano-Fernandez, I., Blain, H.-A., Agustí, J., Piñero, P., Barsky, D., Ivorra, J.,
779 Bourguignon, L., 2019. New clues about the late Early Pleistocene peopling of western
780 Europe: Small vertebrates from The Bois-de-Riquet archeo-paleontological site
781 (Lézignan-La-Cèbe, southern France). *Quat. Sci. Rev.* 219, 187–203.

782 Luzi, E., Pazonyi, P., López-García, J.M., 2019. The influence of climate on
783 morphometric traits of fossil populations of *Microtus arvalis* and *M. agrestis* from the
784 Carpathian Basin, northern Hungary. *Lethaia* 52, 123–132.

785 Macaluso, L., Wencker, L., Castrovilli, M., Carnevale, G., Delfino, M., 2023 A
786 comparative atlas of selected skeletal elements of European urodeles for palaeontological
787 investigations. *Zool. J. Linnean Soc.* 197, 569–619.

788 Mancin, N., Pirini, C., Bicchi, E., Ferrero, E., Valleri, G., 2003. Middle Eocene to Middle
789 Miocene planktonic foraminiferal biostratigraphy for internal basins (Monferrato and
790 northern Apennines, Italy). *Micropaleontology* 49, 341–358.

791 Markova, A.K., 2004. Paleolandscape reconstruction of Likhvin interglacial by the data
792 of Eastern European small mammals. *Izvestia RAN, Seria geograficheskaya* 2, 39–51.

793 Markova, A.K., 2006. Likhvin Interglacial small mammal faunas of Eastern Europe.
794 *Quat. Int.* 149, 67–79.

795 Marquina, R., Fagoaga, A., Crespo, V.D., Ruiz-Sánchez, F.J., Bailon, S., Hernández,
796 C.M., Galván, B., 2017. Amphibians and squamate reptiles from the stratigraphic unit Xb
797 of El Salt (Middle Palaeolithic; Alcoy, Spain): palaeoenvironmental and palaeoclimatic
798 implications. *Spanish J. Palaeontol.* 32, 219–312.

799 Marquina-Blasco, R., Fagoaga, A., Crespo, V.D., Bailon, S., Mallol, C., Hernández,
800 C.M., Galván, B., Ruiz-Sánchez, F.J., 2021. Amphibians and reptiles as
801 palaeoenvironmental proxies during the Late Pleistocene (MIS3): The case of Stratigraphic
802 Unit V of El Salt, Alcoi, Spain. *Palaeogeogr. Palaeoclimatol. Palaeoecol.* 571, 110372.

803 Marquina-Blasco, R., Fagoaga, A., Crespo, V.D., Bailon, S., Mallol, C., Hernández,
804 C.M., Galván, B., Blain, H.-A., Ruiz-Sánchez, F.J., 2022. Applying the UDA-ODA
805 discrimination technique to a herpetological association: the case of the Middle
806 Paleolithic site of El Salt (Alcoi, Spain). *Archaeol. Anthropol. Sci.* 14, 139.

807 Martín-Suárez, E., Freudenthal, M., 1993. Muridae (rodentia) from the lower Turolian of
808 Crevillente (Alicante, Spain). *Scripta Geol.* 103, 65–118

809 Masini, F., Maul, L.C., Abbazzi, L., Petruso, D., 2003. Independent *Arvicola* lineages in
810 Italy and Central Europe?, in: Macholan, M., Bryja, J., Zima, J. (Eds.), Fourth European
811 Congress of Mammalogy, Brno, program and abstracts volume, pp. 164.

812 Masini, F., Maul, L.C., Abbazzi, L., Petruso, D., Savorelli, A., 2020. Independent water
813 vole (*Mimomys savini*, *Arvicola*: Rodentia, Mammalia) lineages in Italy and central
814 Europe. *Foss. Impr.* 76, 59–83.

815 Maul, L.C., Heinrich, W.D., 2007. Neue Daten zur Kleinsäugerbiostratigraphie und
816 Altersabfolge deutscher Quartärfundstellen, *Terra Praehistorica*, in: Festschrift Für
817 Klaus-Dieter Jäger Zum 70. Geburtstag. Beier & Beran, Langenweißbach, pp. 96–110.

818 Maul, L.C., Markova, A.K., 2007. Similarity and regional differences in Quaternary
819 arvicolid evolution in Central and Eastern Europe. *Quat. Int.* 160, 81–99.

820 Maul, L.C., Parfitt, S.A., 2010. Micromammals from the 1995 Mammoth Excavation at
821 West Runton, Norfolk, UK: Morphometric data, biostratigraphy and taxonomic
822 reappraisal. *Quat. Int.* 228, 91–115.

823 Maul L., Masini F., Abbazzi L., Turner A., 1998. The use of different morphometric data
824 for absolute age calibration of some South and Middle European arvicolid populations.
825 *Palaeontogr. Ital.* 85, 111–151.

826 Maul, L.C., Rekovets, L., Heinrich, W.-D., Keller, T., Storch, G., 2000. *Arvicola*
827 *mosbachensis* (Schmidtgen 1911) of Mosbach 2: a basic sample for the early evolution
828 of the genus and a reference for further biostratigraphical studies. *Senckenberg. Lethaea*
829 80, 129–147.

830 Nadachowski, A., 1982. Late Quaternary Rodents of Poland with special reference to
831 morphotype dentition analysis of voles. *Pánstw. Wyd. Nauk.*, Warszawa-Kraków 1–108.

832 Nadachowski, A., 1984. Taxonomic value of anteroconid measurements of M1 in
833 common and field voles. *Acta Theriol.* 29, 123–127.

834 Nadachowski, A., 1989. Origin and history of the present rodent fauna in Poland based
835 on fossil evidence. *Acta Theriol.* 34, 37–53.

836 Nadachowski, A., Zarski, M., Urbanowski, M., Wojtal, P., Miekina, B., Lipecki, G.,
837 Ochman, K., Krawczyk, M., Jakubowski, G., Tomek, T., 2009. Late Pleistocene
838 environment of the Czestochowa Upland (Poland) reconstructed on the basis of faunistic
839 evidence from archaeological cave sites. Institute of Systematics and Evolution of
840 Animals, Polish Academy of Sciences, Kraków, 106 pp.

841 Paunescu, A.C., Maul, L.C., Masini, F., 2004. Comparison of evolutionary patterns of
842 *Arvicola* in Germany, France and Italy, in: Maul, L.C., Kahke, R.-D. (Eds.), 18th
843 International Senckenberg Conference 2004 in Weimar. *Terra Nostra*, pp. 203–204.

844 Petronio, C., Bellucci, L., Martiinetto, E., Pandolfi, L., Salari, L., 2011. Biochronology
845 and palaeoenvironmental changes from the Middle Pliocene to the Late Pleistocene in
846 Central Italy. *Geodiversitas* 33, 485–517.

847 Petruso, D., Locatelli, E., Surdi, G., Valle, C.D., Masini, F., Sala, B., 2011. Phylogeny
848 and biogeography of fossil and extant *Microtus (Terricola)* (Mammalia, Rodentia) of
849 Sicily and the southern Italian peninsula based on current dental morphological data.
850 *Quat. Int.* 243, 192–203.

851 Piñero, P., Agustí, J., 2019. The rodent succession in the Sifón de Librilla section (Fortuna
852 Basin, SE Spain): implications for the Mio-Pliocene boundary in the Mediterranean
853 terrestrial record. *Hist. Biol.* 31, 279–321.

854 Piñero, P., Agustí, J., Blain, H.-A., Laplana, C., 2016. Paleoenvironmental reconstruction
855 of the Early Pleistocene site of Quibas (SE Spain) using a rodent assemblage. *C. R.
856 Palevol* 15, 659–668.

857 Piñero, P., Agustí, J., Oms, O., 2018. The late Neogene rodent succession of the Guadix-
858 Baza Basin (south-eastern Spain) and its magnetostratigraphic correlation. *Palaeontology*
859 61, 253–272.

860 Piñero, P., Agustí, J., Oms, O., Blain, H.-A., Furió, M., Laplana, C., Sevilla, P., Rosas,
861 A., Vallverdú, J., 2020. First continuous pre-Jaramillo to Jaramillo terrestrial vertebrate
862 succession from Europe. *Sci. Rep.* 10, 1–11.

863 Piñero, P., Agustí, J., Laborda, C., Duval, M., Zhao J.-x., Blain, H.-A., Furió, M., Laplana,
864 C., Rosas, A., Sevilla, P., 2022. Quibas-Sima: a unique 1 Ma-old vertebrate succession in
865 southern Iberian Peninsula. *Quat. Sci. Rev.* 283, 107469

866 Railsback, L.B., Gibbard, P.L., Head, M.J., Voarintsoa, N.R.G., Toucanne, S., 2015. An
867 optimized scheme of lettered marine isotope substages for the last 1.0 million years, and
868 the climatostratigraphic nature of isotope stages and substages. *Quat. Sci. Rev.* 111, 94–
869 106.

870 Rekovets, L.I., 1990. La localité Bolchévik 2 et l'évolution de la microthériofaune Au
871 Pléistocène dans la région septentrionale de la Mer Noire. *L'Anthropologie* 94, 659–674.

872 Rekovets, L.I., 1994. Small Mammals of the Anthropogene of the South of Eastern
873 Europe. *Naukova Dumka*, Kiev, 370 pp.

874 Rekovets, L.I., Nadachowski, A., 1995. Pleistocene voles (Arvicolidae) of the Ukraine.
875 *Paleontol. i Evol.* 28–29, 145–245.

876 Reumer, J.W.F., 1984. Ruscinian and early Pleistocene Soricidae (Insectivora,
877 Mammalia) from Tegelen (The Netherlands) and Hungary. *Scripta Geol.* 73, 1–173.

878 Roggero, D., 2003. L'attività estrattiva a Casale e in Monferrato “La Pietra da Cantoni”,
879 in: Violanti, D., Martinetto, E., Pavia, M. (Eds.), *Giornate di Paleontologia 2003. Guida*
880 *alle Escursioni.* 2° ediz. Dip. Scienze della Terra, Torino, 59 pp.

881 Roucoux, K.H., Tzedakis, P.C., de Abreu, L., Shackleton, N.J., 2006. Climate and
882 vegetation 180,000 to 345,000 years ago recorded in a deep-sea core off Portugal. *Earth*
883 *Planet. Sci. Lett.* 249, 307–325

884 Roucoux, K.H., Tzedakis, P.C., Frogley, M.R., Lawson, I.T., Preece, R.C., 2008.
885 Vegetation history of the marine isotope stage 7 interglacial complex at Ioannina, NW
886 Greece. *Quat. Sci. Rev.* 27, 1378–1395.

887 Roucoux, K.H., Tzedakis, P.C., Lawson, I.T., Margari, V., 2011. Vegetation history of
888 the penultimate glacial period (Marine isotope stage 6) at Ioannina, north-west Greece. *J.*
889 *Quat. Sci.* 26, 616–626.

890 Royer, A., García Yelo, B.A., Laffont, R., Hernández-Fernández, M., 2020. New
891 bioclimatic models for the quaternary palaeartic based on insectivore and rodent
892 communities. *Palaeogeogr. Palaeoclimatol. Palaeoecol.* 560, 110040.

893 Saavedra, B., Simonetti, J.A., 1998. Small mammal taphonomy: intraspecific bone
894 assemblage comparison between South and North American Barn Owl, *Tyto alba*,
895 Populations. *J. Archaeol. Sci.* 25, 165–170.

896 Sala, B., 1980. Interpretazione crono-bio-stratigrafica dei depositi pleistocenici della
897 Grotta del Broion (Vicenza). *Geogr. Fis. Dinam. Quatern.* 3, 66–71.

898 Sala, B., Masini, F., 2007. Late Pliocene and Pleistocene small mammal chronology in
899 the Italian peninsula. *Quat. Int.* 160, 4–16.

900 Sánchez-Bandera, C., Fagoaga, A., Serrano-Ramos, A., Solano-García, J., Barsky, D.,
901 DeMiguel, D., Ochando, J., Saarinen, J., Piñero, P., Lozano-Fernández, I., Courtenay,
902 L.A., Titton, S., Luzón, C., Bocherens, H., Yravedra, J., Fortelius, M., Agustí, J., Carrión,
903 J.S., Oms, O., Blain, H.-A., Jiménez-Arenas, J.M., 2023. Glacial/interglacial climate
904 variability in southern Spain during the late Early Pleistocene and climate backdrop for
905 early *Homo* in Europe. *Palaeogeogr. Palaeoclimatol. Palaeoecol.* 625, 111688

906 Sánchez-Goñi, M.F., Bakker, P., Desprat, S., Carlson, A.E., van Meerbeeck, C.J., Peyron,
907 O., Naughton, F., Fletcher, W.J., Eynaud, F., Rossignol, L., Renssen, H., 2012. European
908 climate optimum and enhanced Greenland melt during the Last Interglacial. *Geology* 40,
909 627–630.

910 Sanchiz, B., 1998. *Handbuch der Paläoherpetologie*, 4 Salientia. Friedrich Pfeil,
911 München, 275 pp.

912 Sillero, N., Campos, J., Anna Bonardi, A., Corti, C., Creemers, R., Crochet, P.-A.,
913 Isalovic, J.C., Denoël, M., Ficetola, G.F., Gonçalves, J., Kuzmin, S., Lymberakis, P., de
914 Pous, P., Rodríguez, A., Sindaco, R., Speybroeck, J., Toxopeus, B., Vieites, D.R., Vences,
915 M., 2014. Updated distribution and biogeography of amphibians and reptiles of Europe.
916 *Amphibia- Reptilia* 35, 1–30.

917 Sinitisa, M.V., Pogodina, N.V., 2019. The evolution of early *Spermophilus* in eastern
918 Europe and the antiquity of the Old World ground squirrels. *Acta Palaeontol. Pol.* 64,
919 643–667.

920 Socha, P., 2014. Rodent palaeofaunas from Biśnik Cave (Kraków-Częstochowa Upland,
921 Poland): palaeoecological, palaeoclimatic and biostratigraphic reconstruction. *Quat. Int.*
922 326, 64–81.

923 Speybroeck, J., Beukema, W., Dufresnes, C., Fritz, U., Jablonski, D., Lymberakis, P.,
924 Martínez-Solano, I., Razzetti, E., Vamberger, M., Vences, M., Vörös, J., Crochet, P.-A.,
925 2020. Species list of the European herpetofauna – 2020 update by the Taxonomic
926 Committee of the Societas Europaea Herpetologica. *Amphibia-Reptilia* 41, 139–189.

927 Szyndlar, Z., 1984. Fossil snakes from Poland. *Acta Zool. Cracov.* 28, 1–156.

928 Terry, R.C., 2004. Owl pellet taphonomy: a preliminary study of the post-regurgitation
929 taphonomic history of pellets in a temperate forest. *Palaios* 19, 497–506.

930 Tosetto, V., Damarco, P., Daniello, R., Pavia, M., Carnevale, G., Bisconti, M., 2023.
931 Cranial material of long-snouted dolphins (Cetacea, Odontoceti, Eurhinodelphinidae)
932 from the Early Miocene of Rosignano Monferrato, Piedmont (NW Italy): anatomy,
933 paleoneurology, phylogenetic relationships and paleobiogeography. *Diversity* 15, 227.

934 Valde-Nowak, P., Nadachowski, A., 2014. Micoquian assemblage and environmental
935 conditions for the Neanderthals in Obłazowa Cave, Western Carpathians, Poland. *Quat.*
936 *Int.* 326-327, 146–156.

937 Van de Weerd, A., 1976. Rodent faunas of the Mio-Pliocene continental sediments of the
938 Teruel-Alfambra region, Spain. *Utrecht Micropaleontol. Bull.* 2, 1–217.

939 Van der Meulen, A., 1973. Middle Pleistocene smaller mammals from the Monte Peglia,
940 (Orvieto, Italy) with special reference to the phylogeny of *Microtus* (Arvicolidae,
941 rodentia). *Quaternaria* 17, 1–114.

942 van Kolfschoten, T., 1990. The evolution of the mammal fauna in the Netherlands and
943 the Middle Rhine area (Western Germany) during the late Middle Pleistocene. *Med. Rijks*
944 *Geol. Dienst* 43, 1–69.

945 van Kolfschoten, T., Turner, E., 1992. Early Middle Pleistocene mammalian faunas from
946 Kärlich and Miesenheim I and their biostratigraphical implications, in: Turner, E. (Ed.),
947 *The Early Middle Pleistocene in Europe*, Rotterdam, pp. 227–253.

948 Villa, A., Delfino, M., 2019. A comparative atlas of the cranial osteology of European
949 lizards (Reptilia, Squamata). *Zool. J. Linnean Soc.* 187, 828–928.

950 Villa, P., Soriano, S., Grün, R., Marra, F., Nomade, S., Pereira, A., Boschian, G.,
951 Pollarolo, L., Fang, F., Bahain, J.J., 2016. The Acheulian and early Middle Paleolithic in
952 Latium (Italy): stability and innovation. *PLoS One* 11(8), e0160516.

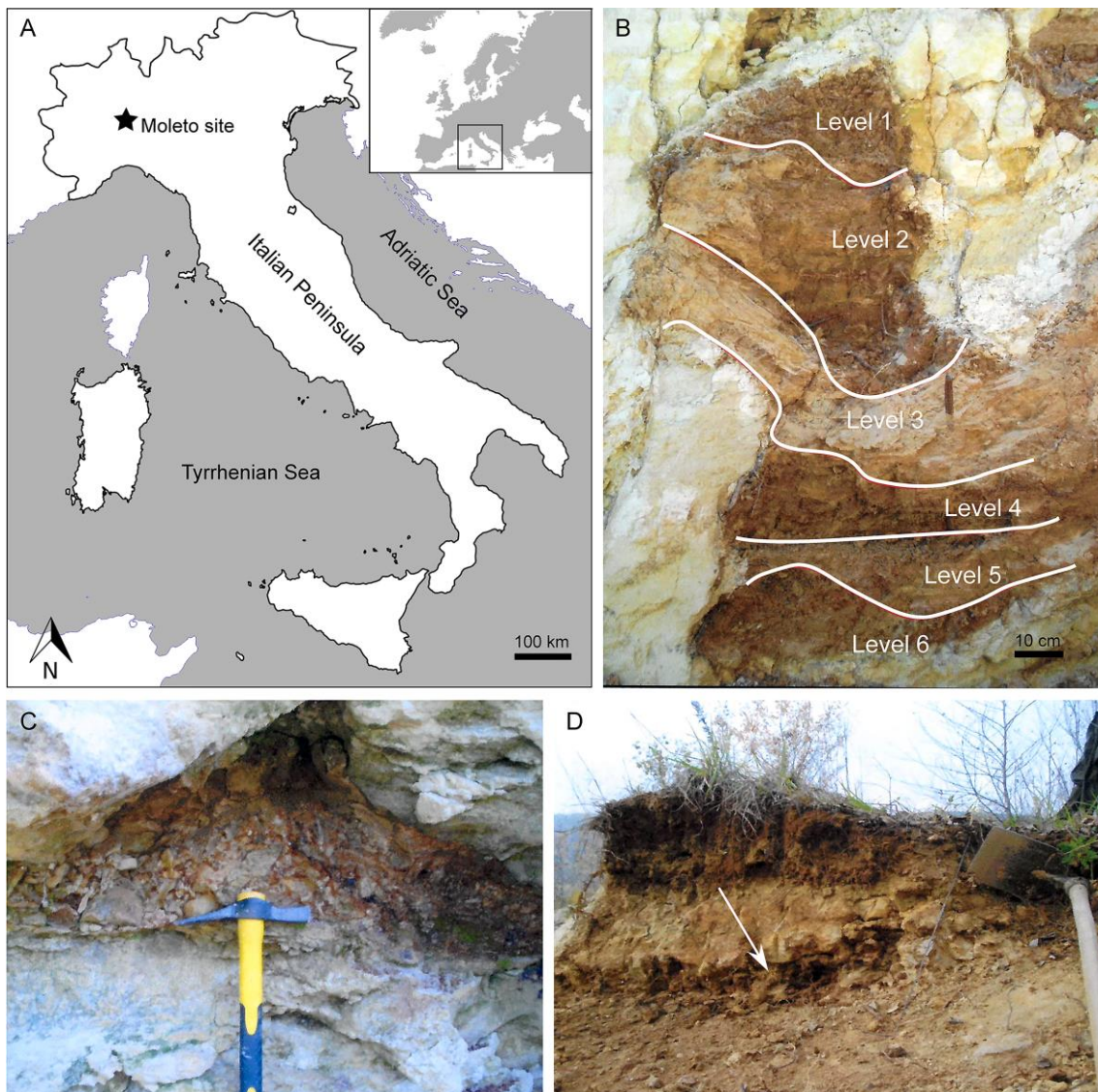
953 Vogrin, M., Corti, C., Pérez Mellado, V., Sá-Sousa, P., Cheylan, M., Pleguezuelos, J.,
954 Meyer, A., Schmidt, B., Sindaco, R., Romano, A., Martinez Solano, I., 2009. *Hierophis*
955 *viridiflavus*. The IUCN Red List of Threatened Species 2009: e.T61449A86246670.
956 <http://dx.doi.org/10.2305/IUCN.UK.2009.RLTS.T61449A12487580.en>

957 von Koenigswald, W., 1973. Veränderungen in der Kleinsäugerfauna von Mitteleuropa
958 zwischen Cromer und Eem (Pleistozän). *Eiszeitalter und Gegenwart* 23/24, 159–167.

959 von Koenigswald, W., 1980. Schmelzstruktur Und Morphologie in dem molaren der
960 Arvicoliden (Rodentia). *Abhandlungen Senckenberg Naturforschung Gesellschaft* 59, 1–
961 94.

962 von Koenigswald, W., van Kolfschoten, T., 1996. The *Mimomys*–*Arvicola* boundary and
963 the enamel thickness quotient (SDQ) of *Arvicola* as stratigraphic markers in the Middle
964 Pleistocene, in: The Early Middle Pleistocene in Europe. Balkema, pp. 211–238.

965 **Figures**



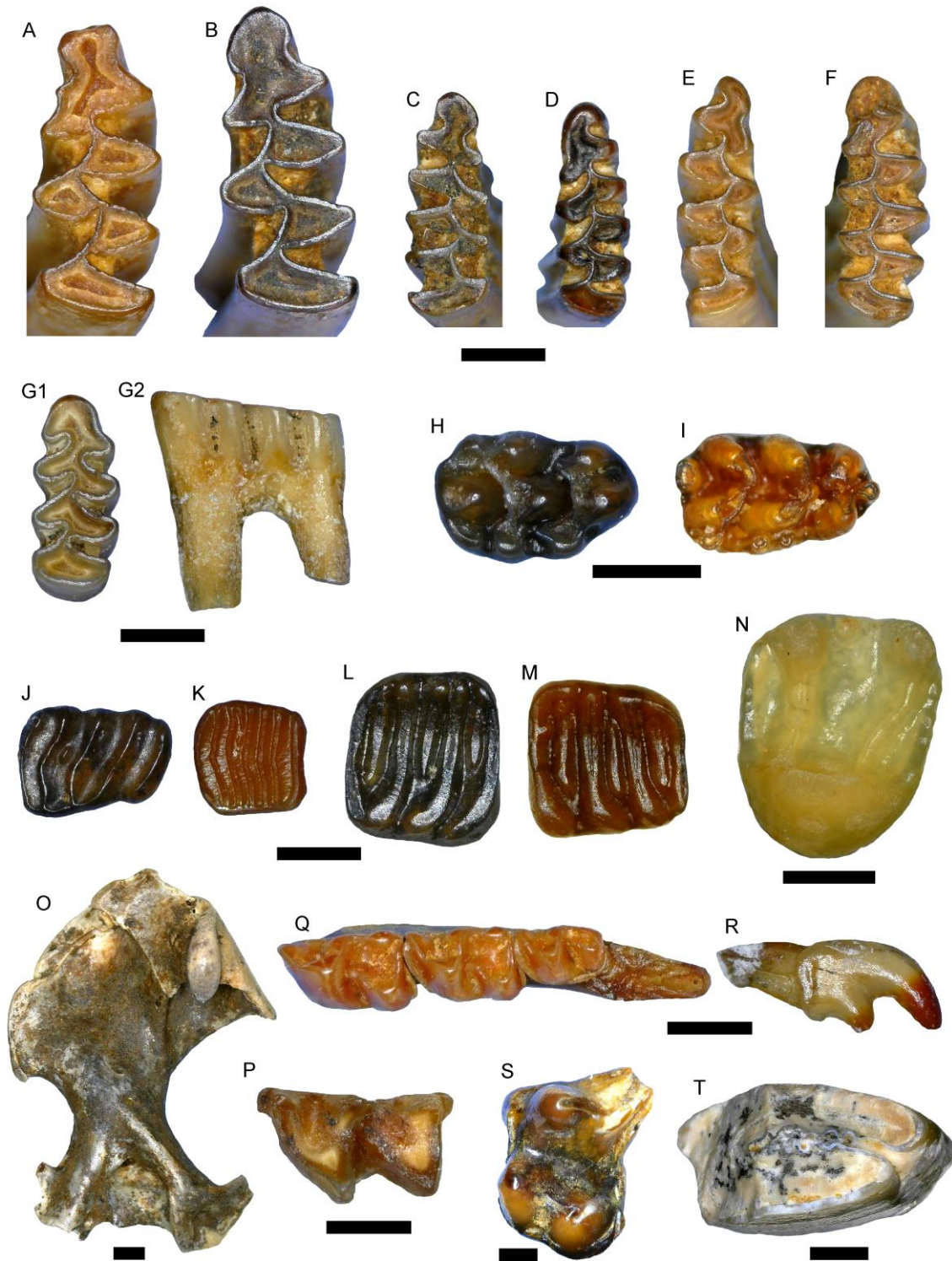
966

967 **Figure 1.** Geographic and stratigraphic context. A, Location of the Moieto site (source:
968 Google Earth Pro). B, Section of Moieto 1 showing six different levels. C, Fissure of
969 Moieto 0. D, Moieto 2 with the arrow pointing to the fossiliferous deposit. [2-column]



970

971 **Figure 2.** Digital images of amphibians, squamate reptiles, and birds from Moletó.
 972 *Salamandra salamandra*: A, trunk vertebra in dorsal view, MGPT-PU 142439. *Bufo* gr.
 973 *bufo*: B, right ilium in lateral view, MGPT-PU 142447. *Rana* sp.: C, right humerus in
 974 ventral view, MGPT-PU 142448. *Anguis* gr. *fragilis*: D, osteoderm in external view,
 975 MGPT-PU 142445. Lacertidae indet.: E, fragment of right maxilla in medial view,
 976 MGPT-PU 142442. *Hierophis* sp.: F, trunk vertebra in ventral view, MGPT-PU 142443.
 977 *Natrix* sp.: G, trunk vertebra in left lateral view, MGPT-PU 142525. *Vipera* gr. *aspis*: H,
 978 trunk vertebra in anterior view, MGPT-PU 142449. Passeriformes indet.: I, right
 979 tibiotarsus in cranial view, MGPT-PU 130648. Scale bars equal 1 mm (A–C and F–I) or
 980 0.5 mm (D and E). [2-column]



981

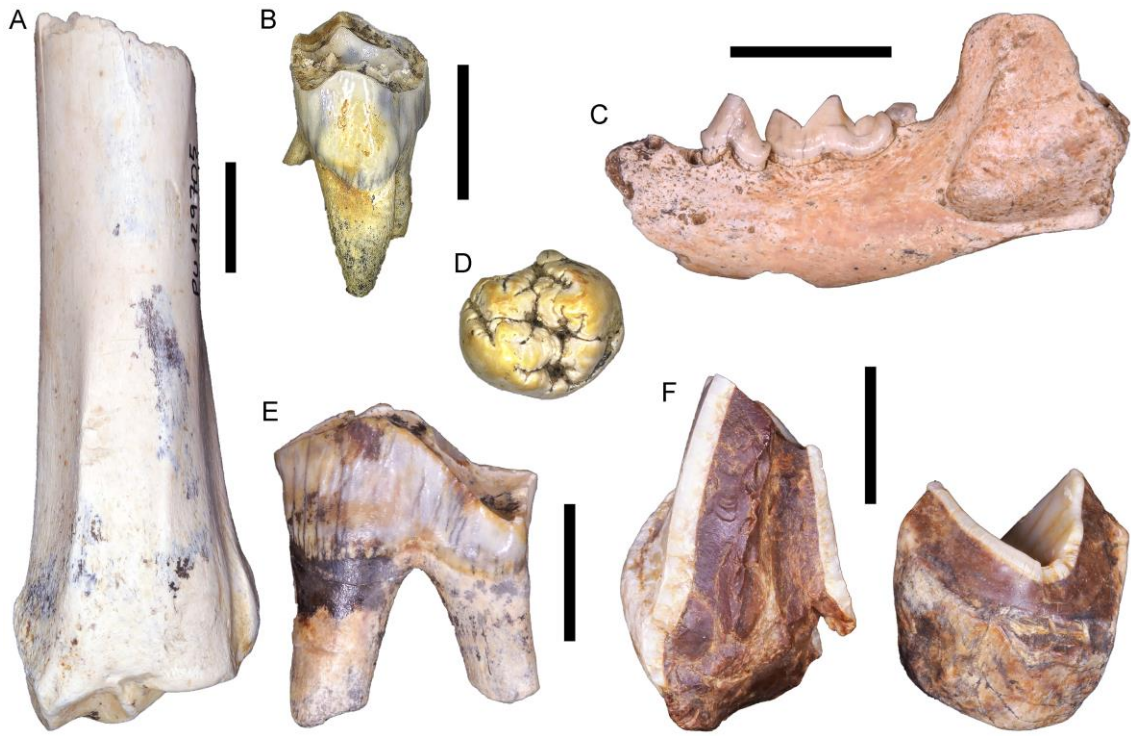
982 **Figure 3.** Digital images of small mammals from Moletto. *Arvicola mosbachensis*: A, left
 983 m1 from Moletto 0, MGPT-PU 129539; B, left m1 from Moletto 0, MGPT-PU 129538.
 984 *Microtus (Terricola) gr. multiplex-subterraneus*: C, right m1 from Moletto 0, MGPT-PU
 985 129543; D, left m1 from Moletto 1, MGPT-PU 129604. *Microtus (Agricola) cf. agrestis*:

986 E, right m1 from Moletto 0, MGPT-PU 129544. *Microtus (Microtus) cf. arvalis*: F, left
987 m1 from Moletto 0, MGPT-PU 129545. *Clethrionomys glareolus*: G, left m1 from Moletto
988 1, in occlusal (1) and lateral (2) views. *Apodemus gr. sylvaticus-flavicollis*: H, right M1
989 from Moletto 1, MGPT-PU 129627; I, right m1 from Moletto 1, MGPT-PU 129650.
990 *Muscardinus avellanarius*: J, right M1 from Moletto 1, MGPT-PU 129583; K, right M2
991 from Moletto 1, MGPT-PU 129597. *Glis glis*: M, right M2 from Moletto 2, MGPT-PU
992 129665; N, right m1 from Moletto 2, MGPT-PU 129664. *Sciurus sp.*: O, left M1/2 from
993 Moletto 1, MGPT-PU 129568. *Talpa europaea*: P, right humerus from Moletto 0, MGPT-
994 PU 129504; Q, left m2 from Moletto 2, MGPT-PU 129663. *Sorex sp.*: R, left mandible
995 with m1, m2 and m3 from Moletto 0, MGPT-PU 129503; S, right I1 from Moletto 0,
996 MGPT-PU 129502. *Erinaceus europaeus*: T, right P4 from Moletto 0, MGPT-PU 129500.
997 Lagomorpha indet: M, left P3 from Moletto 0, MGPT-PU 129505. Scale bars equal 1 mm.

998 [2-column]

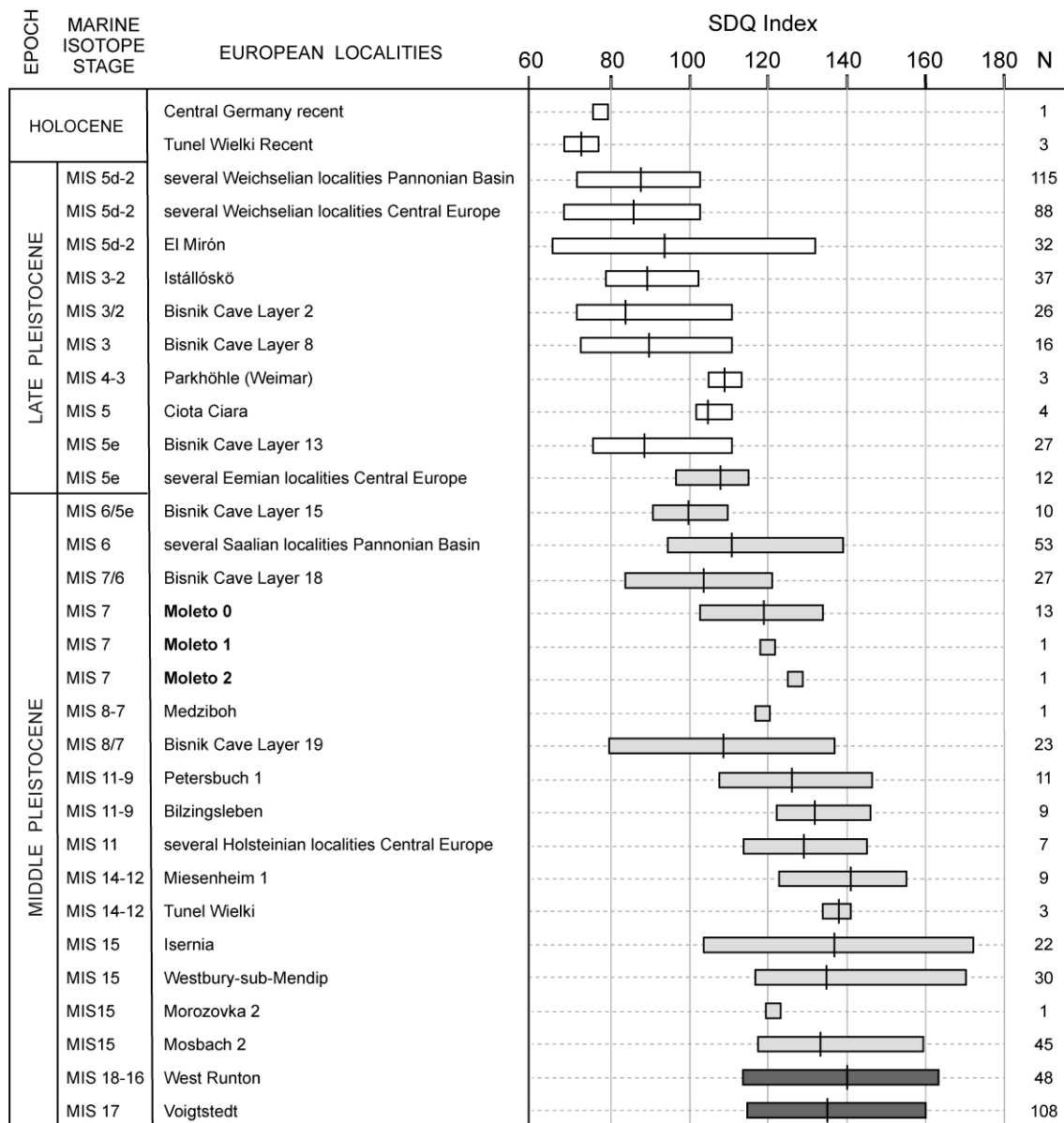
999

1000



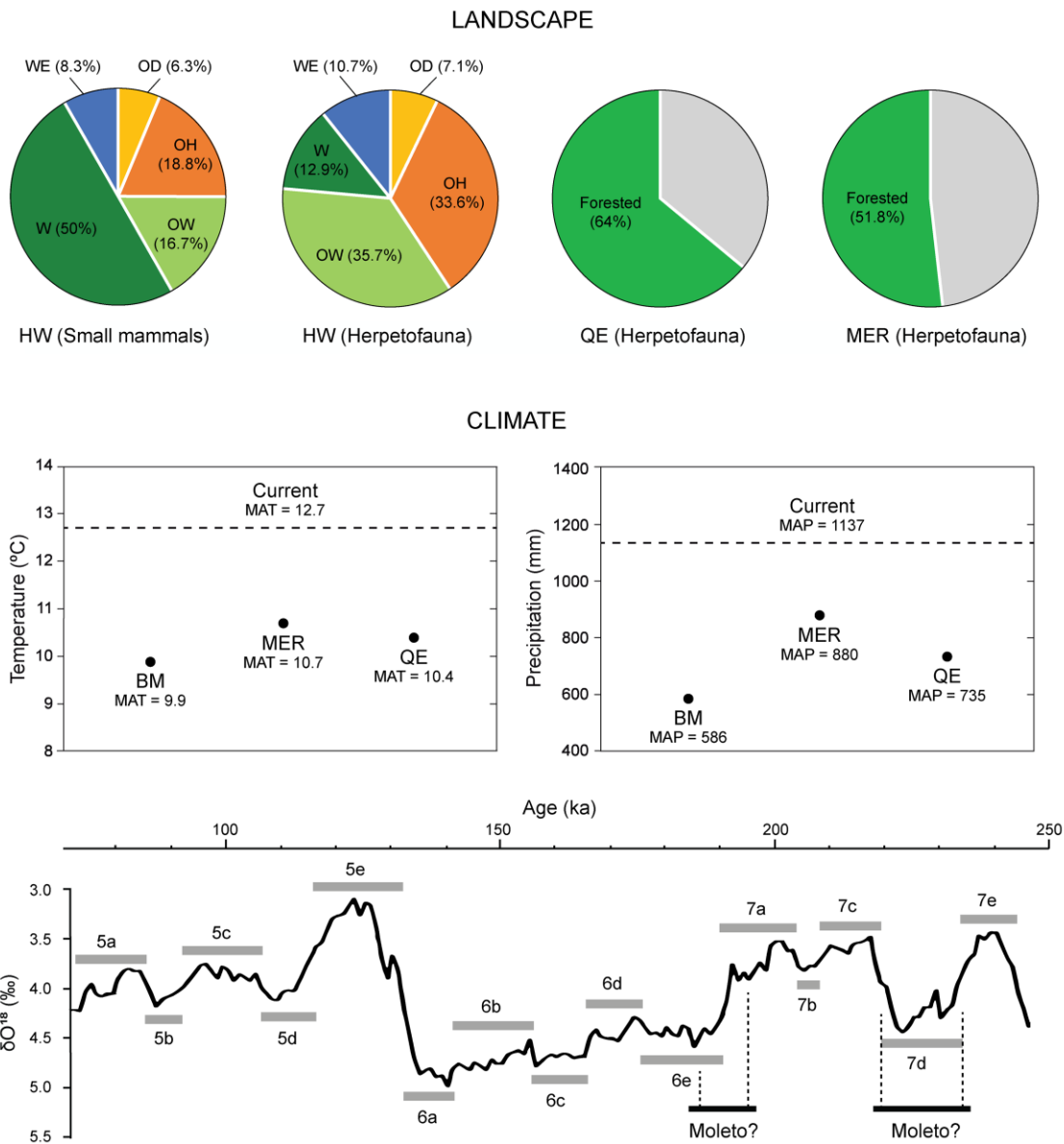
1001

1002 **Figure 4.** Digital images of large mammals from Moletto. *Capreolus capreolus*: A, left
 1003 distal radius in dorsal view, MGPT-PU 129705. *Dama cf. dama*: B, left P4 in palatal
 1004 view, MGPT-PU 129694. *Mustela putorius*: C, left hemimandible in labial view, MGPT-
 1005 PU 129699. *Sus cf. scrofa*: D, indeterminate upper molar in occlusal view, MGPT-PU
 1006 129696. *Cervus elaphus*: E, left p2 in labial view, MGPT-PU 129695. *Stephanorhinus*
 1007 sp.: F, fragments of upper molar, MGPT-PU 129698. Scale bars equal 10 mm. [2-column]



1008 *Arvicola amphibius* (or *A. terrestris*) *Arvicola mosbachensis* (or *A. cantianus*) *Mimomys savini*

1009 **Figure 5.** Enamel thickness quotient (SDQ) values of Middle Pleistocene and Late
 1010 Pleistocene *Mimomys* and *Arvicola* from Europe. A decreasing trend in SDQ can be
 1011 observed from late populations of *Mimomys savini* to late populations of *Arvicola*. The
 1012 chronological assignment and the SDQ values have been taken from Heinrich (1982), van
 1013 Kolfschoten and Turner (1992), Rekovets and Nadachowski (1995), Maul et al. (1998),
 1014 Maul and Heinrich (2007), Cuenca-Bescós et al. (2010), Maul and Parfitt (2010), Socha
 1015 (2014), Berto et al. (2016, 2021), Luzi et al. (2019), and this work. N, number of
 1016 specimens. [2-column]



1022

1023 **Figure 7.** Landscape and climate values obtained with the small mammal and
 1024 herpetofauna assemblages from Moleto and possible location of the site in the scheme of
 1025 marine isotope substages (modified from Railsback et al., 2015). BM, Bioclimatic Model;
 1026 QE, Quantified Ecology; HW, Habitat Weightings; MAT, mean annual temperature;
 1027 MAP, mean annual precipitation; MER; Mutual Ecogeographic Range; OD: open dry
 1028 meadows or shrublands; OH: open humid meadows; OW: open woodland; W: woodland
 1029 and woodland-margin areas; WE: water-edges. [2-column]

1030

1031 **Table captions**

1032 **Table 1.** Vertebrate faunal list of the site of Moletto.

1033 **Table 2.** Relative abundances of small mammals (rodents and insectivores) and
1034 herpetofauna (amphibians and squamate reptiles) from the late Middle Pleistocene site of
1035 Moletto, with the distribution of their potential habitats. W: woodland and woodland-
1036 margin areas; OD: open dry meadows or shrublands; OH: open humid meadows; OW:
1037 open woodland; WE: water-edges.

1038 **Table 3.** Palaeoenvironmental results (% forested) obtained from Quantified Ecology
1039 (Jeannet, 2010) on the amphibian and squamate reptile assemblages from Moletto. SD:
1040 Standard deviation.

1041 **Table 4.** Palaeoclimatic results obtained from Quantified Ecology (Jeannet, 2010) on the
1042 amphibian and squamate reptile assemblages from Moletto. As modern reference, we used
1043 the data of climate-data.org giving 12.7 °C for MAT, 1137 mm for MAP, 1.7 °C for MTC,
1044 and 23.8 °C for MTW. SD: Standard deviation; Δ : anomaly in relation to present climate.

1045 **Table 5.** Results obtained from Mutual Ecogeographic Range (Blain et al., 2009, 2016)
1046 using UDA-ODA technique (Fagoaga et al., 2019) on the amphibian and squamate reptile
1047 assemblages from Moletto. As modern reference, we used the data from WorldClim 2.1
1048 giving 12.1 °C for MAT and 843.1 mm for MAP (Fick and Hijmans, 2017). SD: Standard
1049 deviation; Δ : anomaly in relation to present climate. MAT: mean annual temperature;
1050 MAP: mean annual precipitation; MTC: mean temperature of the coldest month; MTW:
1051 mean temperature of the warmest month; percentage wood: extension of wooded areas.
1052 MAT, MAP, MTC, and MTW are in °C, whereas percentage wood is expressed in %.

1053 **Table 6.** Climatic parameters for Moleto calculated according to the bioclimatic analysis
1054 based on rodent and insectivore associations proposed by Hernández Fernández (2001),
1055 and present climate data from the area (Climate-data.org). Δ : Difference between results
1056 and current data; MAT: mean annual temperature (in °C); MTW: mean temperature of
1057 the warmest month (in °C); MTC: mean temperature of the coldest month (in °C); MAP:
1058 mean annual precipitation (in mm); SD: standard error for the estimation.

1059 **Table 7.** Distribution of the rodent and insectivore species identified at Moleto according
1060 to their climate preferences, in accordance with Hernández-Fernández (2001) and
1061 Hernández-Fernández et al. (2007). IV, Subtropical with winter rains and summer
1062 droughts; VI, Typical temperate; VII, Arid-temperate; VIII, Cold temperate (boreal) and
1063 IX, Polar. *For *Sciurus* sp. we have used the distribution of *Sciurus vulgaris*.

1064